Journal of Water Process Engineering 49 (2022) 103076

Contents lists available at ScienceDirect

Journal of Water Process Engineering

journal homepage: www.elsevier.com/locate/jwpe

Insights on the hydrogel-forming ability and post-gelling mechanical properties of structural extracellular polymeric substances (sEPS) from aerobic granular sludge (AGS): A comparison with model biopolymers

Benedetta Pagliaccia [a,b], Sidonie Durieux [a], Yolaine Bessiere [a,*], Mansour Bounouba [a], Abdo Bou Sarkis [a,c], Elisabeth Girbal-Neuhauser [c], Emiliano Carretti [d], Claudio Lubello [b], Tommaso Lotti [b], Etienne Paul [a]

[a] TBI, Université de Toulouse, CNRS, INRAE, INSA, 35 avenue de Rangueil, 31077 Toulouse, France
[b] Department of Civil and Environmental Engineering (DICEA), University of Florence, Via di Santa Marta 3, 50139 Firenze, FI, Italy
[c] Laboratoire de Biotechnologies Agroalimentaire et Environnementale (LBAE), UPS, Université de Toulouse, 24 rue d'Embaquès, 32000 Auch, France
[d] Department of Chemistry "Ugo Schiff" & CSGI, University of Florence, Via della Lastruccia 3 – 13, 50019 Sesto Fiorentino, FI, Italy

ARTICLE INFO

Keywords:
Extracellular polymeric substances
Aerobic granular waste sludge
Resource recovery
Hydrogel
Methodology
Rheology

ABSTRACT

The hydrogel-forming ability and post-gelling mechanical properties of structural extracellular polymeric substances (sEPS) extracted from aerobic granular sludge (AGS) were studied in comparison to well-known biopolymers (i.e., alginate and κ-/ι-carrageenan) taking advantage of material-saving, reproducible and robust experimental protocols.

With respect to alginate and κ-carrageenan, sEPS and ι-carrageenan hydrogels formed in presence of divalent metal ions M^{2+} behaved similarly once subjected to consecutive compression-decompression cycles, deforming elastically in all the applied range of deformations. While the overall mechanical response remained almost unchanged varying polymer concentration and ionic cross-linker concentration and nature, the Young's modulus E appeared significantly affected by the applied gelling conditions ($E \simeq$ 4–20 kPa). As a result of the higher complexity of the extracellular biopolymeric matrix, higher driving forces (sEPS and M^{2+} concentrations) were needed to form stable and stiff hydrogels with respect to the studied model biopolymers: the establishment of an extended 3D network started for sEPS concentrations around 2.5 wt% ($Ca^{2+} \geq 0.1$ M). Oscillatory shear experiments confirmed that sEPS were able to form hydrogels with solid-like mechanical properties at 1–10 wt% sEPS concentrations. Overall, the optimization of the gelling methods performed might help to overcome many bottlenecks characterizing this research area. The feasibility of forming sEPS hydrogels with mechanical properties comparable to other biopolymer-based systems currently applied for commercial purposes led to an awareness of the potential application and might open new valorisation scenarios able to contribute to a more bio-based and circular economy.

1. Introduction

Aerobic granular sludge (AGS) technology is a promising and viable alternative to conventional activated sludge (CAS) systems for biological wastewater treatment [1]. The compact granular form provides better settling properties, a more effective sludge–effluent separation and a higher biomass retention and facilitates the simultaneous removal of chemical oxygen demand (COD), nitrogen (N) and phosphorus (P) [2–6]. These advantages allow running wastewater treatment plants (WWTPs) that require up to 30 % less energy input and 75 % less space occupation combined with significant lower investment costs [7]. AGS-based processes are currently applied in the water line of both municipal and industrial WWTPs: intensive research effort has been dedicated in the last decade on the technology optimization and a comprehensive literature was produced studying the AGS performance and operation strategies in laboratory- and/or pilot-scale sequencing batch reactors (SBR) [2,8,9]. Furthermore, the combination of membrane bioreactor (MBR) with AGS (AGS-MBR) has been studied to improve the treatment

* Corresponding author.
E-mail address: yolaine.bessiere@insa-toulouse.fr (Y. Bessiere).

https://doi.org/10.1016/j.jwpe.2022.103076
Received 9 June 2022; Received in revised form 22 July 2022; Accepted 15 August 2022
Available online 24 August 2022

efficiency and overcome the shortcomings of the MBR technology: indeed, AGS has been proven to have a low fouling potential in such reactors [10,11].

As in conventional biofilms, in AGS microorganisms produce a significant amount of highly hydrated extracellular polymeric substances (EPS) to form a hydrogel matrix in which they are self-immobilized [12–14]. EPS are a complex mixture of polysaccharides, proteins, nucleic acids, (phospho)lipids, humic substances, etc. [12–15]. EPS contribute to the initial aggregation of microbial cells [12] as well as to the architectural structure, rheological behaviour and functional stability of granules, thus influencing the physical-chemical properties of the biomass catalyzing the biological treatment process. Particularly, EPS have been demonstrated to exert various important functions in the bioaggregates, such as a protective barrier against detrimental environment, maintenance of a stable structure, settling properties, surface charge, protection against dehydration, nutrient source, and organic substance sorption capacity [14,16].

Aerobic granules contain EPS with gel-forming properties (up to about 25 wt% of the organics originally present in the biomass [17]): particularly, these AGS-derived EPS have the ability to form hydrogels with calcium ions after being extracted and they are previously denominated in literature as alginate-like exopolysaccharides or ALE due to the chemical and functional similarities with alginate [18]. Indeed, both are alkaline extracted, form stable hydrogels with calcium ions, precipitate as gels at acidic pH and are rich in carboxyl groups [18–20]. However, the higher complexity of sEPS with respect to alginate has been proved by follow-up research [20]. These EPS are considered to be strongly involved in the structural integrity of aerobic granules [17], and hence they are currently referred to as structural EPS (sEPS).

The environmental and economic sustainability of wastewater treatment may be enhanced by the EPS recovery and conversion into bio-based commodities [7]. Indeed, the excess sludge is considered the main waste product in WWTPs and its processing costs account for nearly half of the total operational capital [21]. The recovery of biopolymers like EPS as new cost-effective and high-performance biomaterials would hence promote a more efficient waste sludge management, thus contributing to a perspective shift from WWTPs to water resource recovery facilities (WRRFs) in the circular economy framework [18,22,23]. Thanks to their versatile properties, EPS have been already studied as bio-based products in various environment- and industry-related applications (e.g., water-proof coating in paper industry [7], flame retardant agents [24], additives for cement curing [25], membrane fabrication [26] and biosorbent media [27–29]). However, the implementation of EPS recovery-oriented solutions is currently hampered by many bottlenecks which can be mainly identified in a still incomplete understanding of the EPS properties as well as in the poor regulation of the EPS production depending on the specific research/applicative goals. As highlighted by Seviour et al. [14], structural and functional assignment of key biofilm-derived EPS (e.g., AGS-extracted sEPS) is confounded by their compositional complexity and interactions as well as by the challenges in processing and isolating the EPS components. The development of sensitive and dedicated methodologic approaches able to shed light on the compositional, physical-chemical, and functional properties (including the hydrogel-forming ability) of AGS-extracted sEPS is hence pivotal to progress towards the broader implementation of resource recovery-oriented solutions.

Hydrogel-like materials are gaining increasingly commercial interest in multiple fields (e.g., agriculture, water purification, biomedicine, food industry, personal hygiene) thanks to their excellent properties of water-holding ability, slow-release capacity, softness, etc. Particularly, in line with the growing environmental awareness which leads the scientific community to embrace a “green” thinking, the attention has been gradually shifted from petroleum-derived polymer- to biopolymer-based hydrogels which exhibit the unique advantages of biodegradability, non-toxicity, and relative low-cost [30,31]. In this perspective, the hydrogel-forming ability of AGS-derived sEPS might be engineered in industry- and/or environment-related solutions with high market demand potential, thus contributing to a less fossil fuel-dependent manufacturing sector. The broader implementation of sEPS hydrogel-like materials in miscellaneous sectors is driven by the integrated assessment of many fundamental properties (e.g., mechanical behaviour, physical-chemical features, biodegradability, chemical resistance and durability, biological stability, etc.) whose level of priority appears strictly dependent on the final use of the designed bioproducts. For instance, the development of sEPS-based biomaterials with high effectiveness in agriculture-related applications (e.g., soil conditioning) imposes high qualitative standards (e.g., absence of phytotoxic elements, low levels of heavy metals, etc.) and capacity to adsorb and hold significant water quantities. Polymer-related applications in agriculture should also feature adequate degradation rates (avoiding soil contamination due to the production of non-biodegradable residues) as well as long-term functionality and stability [32]. In the case of hydrogel-like materials to be applied in the construction sector (e.g., additive to improve the concrete durability) a high chemical resistance (for instance against chemical attacks by acids, chlorine, sulphate) has been emphasized as crucial in addition to great water-binding properties [33]. Regardless of the specific industrial solution, the hydrogel mechanical behaviour has long been recognized as fundamental [34]: its characterization is hence a pre-requisite in exploring existing and potential applications. For example, in water and/or wastewater treatment systems (e.g., heavy metal and organic dye removal [35]), hydrogels are expected to maintain high mechanical standard over time to facilitate the post-treatment separation phase. In agriculture- and/or biomedicine-related solutions, where hydrogels are applied as carrier systems for the delivery and controlled-release of agrochemicals [32] and/or drugs [35], respectively, high stiff and elasticity can be required to protect the encapsulated components from the mechanical deformation. Conversely, weaker hydrogels are demanded for applications as substrates for plant cutting and/or micropropagation in horticulture and nursery sector to not compromise the root growth. The level of the post-gelling mechanical properties is therefore strictly dependent on the targeted application. To be noticed that biopolymer-based hydrogels usually present relatively small elastic modulus values, being constituting of a substantial fraction of water (exerting only viscous features): this could represent a limiting factor in their widespread adoption in many kinds of mechanics-dependent solutions (e.g., tissue engineering) especially if compared with traditional engineering materials [34].

The feasibility of forming hydrogel-like materials with tunable mechanical properties covering a wide range of potential industrial and/or environmental solutions is therefore pivotal. Various factors can affect the polymer post-gelling mechanical properties such as molecular weight distribution, cross-linking density, gelation rate, cross-linking method, environmental conditions (e.g., pH, T, ionic strength), etc. [5,36]. A comprehensive characterization is made even more challenging by the complex nature of the AGS-extracted sEPS. It has been reported that the mechanical properties of ionically cross-linked sEPS hydrogels can be influenced by the origin of the microbial aggregate (for instance in terms of wastewater treated [37]) as well as by the type of metal M^{2+} used as ionic cross-linker [20]. Seviour et al. [5] observed that a weakening of the EPS matrix in AGS is induced by several environmental factors including temperature, pH and ionic strength. Despite these key findings, further work is encouraged to shed light on the impact of the whole production processes (e.g., extraction and gelling methods) on the mechanics of the resulting hydrogels. In this regard, the definition of standard methods for the mechanical testing combining high-effectiveness and minimized polymer consumption gains a crucial role to progress in this relatively recent research field. To be noticed that large part of the experimental studies is carried out using AGS cultivated in laboratory, thus limiting the quantities of available materials. This could become an obstacle for a comprehensive analysis of the sEPS

hydrogel-forming ability, thus making necessary preliminary miniaturization studies.

In this perspective, this work mainly aimed to shed light on the hydrogel-forming ability and post-gelling mechanical properties of AGS-derived sEPS. Methodologic insights to optimize the gelling methods based on the research objectives/constraints were given. Particularly, varying polymer concentrations and ionic cross-linker concentration and nature, the sEPS post-gelling mechanical behaviour was assessed in comparison to well-known biopolymers (i.e., alginate and κ-/ι-carrageenan) via rheometry. More detailed, the stress–strain response to consecutive compression–decompression cycles was addressed varying the above-mentioned gelling conditions, and the resulting Young's modulus *E* was studied as sensitive parameter to point out the mechanical similarities and differences among the studied systems. This comprehensive analysis was mainly employed to evaluate the feasibility of forming hydrogel-like materials with tunable mechanical properties upon variations of the sEPS cross-linking conditions. The choice of alginate and κ-/ι-carrageenan as reference polymers was driven by different reasons. Indeed, all the studied biopolymers (including sEPS) are able to form (ionically cross-linked) hydrogels in presence of metal ions but they differ by their functional groups (e.g., carboxyl groups for alginate and sulphate-half esters for κ-/ι-carrageenan) and gelling mechanisms (e.g., egg-box model for alginate [38–40] and conversion from a random coil to double helix structure below a critical temperature for κ-/ι-carrageenan [41–43]). Alginate has been already studied in comparison with the gel-forming EPS [18,20] and hence considered an appropriate reference. The presence of sulphate groups in AGS-derived sEPS has been reported in literature [20], thus making κ-/ι-carrageenan adequate candidates to strengthen the outcome of the characterization studies. Oscillatory shear measurements were also carried out by varying the sEPS concentrations: coupled with above-described compression studies, these experiments were employed to (i) gain insights on the hydrogel response to another kind of mechanical perturbation and to (ii) suggest additional considerations concerning the hydrogel-forming processes.

Overall, this manuscript proposes a comprehensive analysis on the post-gelling mechanics of AGS-derived sEPS: this would represent a prerequisite in studying potential valorisation strategies for these waste-derived biopolymers, thus paving the way towards the development of sEPS-based products to be applied in multiple fields thanks to their versatile mechanical features.

2. Materials and methods

2.1. AGS-derived sEPS

To validate the developed methodologies on structural EPS (sEPS) from different microbial aggregates, $sEPS_A$ and $sEPS_B$ were extracted from aerobic granules cultivated in two distinct pilot-scale SBRs, R_A and R_B, respectively, whose characteristics are described in *Supplementary material* (Paragraph S1).

The extraction protocol was adapted from Schambeck et al. [37]. In brief, a known amount of dried granules was incubated in 0.2 M Na_2CO_3 (pH 11.3, 32 mL of solvent for each 0.2 g of dried granules; 300 rpm, 30 min) and then homogenized with ultraturrax (Janke & Kunkel from IKA-Labortechnik) at a speed of 13,500 rpm for 3 cycles of 1 min separated by 45 s of resting phases. The disrupted granules were then heated for 60 min in a water bath at 80 °C. After centrifugation (22,000 ×*g*, 15 min, 4 °C), the supernatant, consisting of EPS, was collected. Structural EPS (sEPS) were hence recovered via acidic precipitation by adding 1 M HCl to the (alkaline) EPS dispersion until pH 2.0 ± 0.2 was achieved [18]. After centrifugation (22,000 ×*g*, 15 min, 4 °C), the pellet of sEPS was collected, re-solubilized in 0. 1 M NaOH, dialyzed for 36 h (3.5 kDa molecular weight cut off, MWCO) against distilled water, freeze-dried and finally analyzed for their Volatile Solids (VS) content. The freeze-dried $sEPS_A$ were dissolved in 0.05 M NaOH while $sEPS_B$ needed stronger alkaline conditions for the re-solubilization (0.1–0.2 M NaOH). The obtained sEPS dispersions at various weight concentrations (1–10 wt% sEPS) were applied in the hydrogel-forming experiments.

The extracted sEPS were analyzed through colorimetric assays for the evaluation of proteins, humic acids, uronic acids, and neutral sugars. Particularly, proteins (as Bovine Serum Albumin, BSA, equivalent) and humic acids were estimated according to the modified Lowry method [44], while uronic acids and neutral sugars were determined by means of the double anthrone method [45] as glucuronic acid (Gluc. Acid) and glucose (Glu) equivalents, respectively (Fig. S1 in *Supplementary material*). The extracted sEPS were also analyzed by Fourier Transform-Infrared (FT-IR) spectroscopy using a BioRad FTS-40 spectrometer (4 cm^{-1} resolution, 64 scans, spectral range 2000–400 cm^{-1}, DTGS detector).

2.2. Model biopolymers

The hydrogel-forming ability and post-gelling mechanical behaviour of sEPS were compared to those of well-characterized biopolymers selected as model biopolymers: alginate and κ-/ι-carrageenan. In this regard, an alginic acid from brown algae (*Macrocystis pyrifera*) purchased from Sigma-Aldrich approximately composed by 61 % mannuronic acid (M) and 39 % guluronic acid (G) ($M/G \simeq 1.56$) was dissolved in 0.1 M NaOH with concentrations ranging between 1 and 5 wt% to be then applied in the hydrogel-forming experiments. Conversely, commercial κ- and ι-carrageenan (purchased from Sigma-Aldrich) were dissolved in 0.01 M NaOH with heating at about 65 °C with concentrations ranging between 1 and 5 wt%; the heated κ-/ι-carrageenan dispersions were then subjected to hydrogel-formation upon cooling at room temperature.

2.3. Hydrogel-forming protocol

Limitations due to the low material availability are often addressed by researchers working with AGS from laboratory- and/or pilot-scale reactors. Combining minimized polymer consumption and high accuracy in the characterization studies is therefore challenging. A material-saving hydrogel-forming protocol, characterized by reproducibility, sensitivity and minimized polymer consumption, was therefore adapted from Felz et al. [20]. The biopolymer-based hydrogels were obtained via ionic cross-linking in presence of various divalent metal cations M^{2+} ($M^{2+} = Ca^{2+}$, Cu^{2+}, Ni^{2+}, Mg^{2+}; $M^{2+} = 0.01–1$ M) controlling the cross-linking kinetics through dialysis (3.5 kDa molecular weight cut-off MWCO). The hydrogel geometry was controlled by forcing the sol-gel transition in a fixed cylindrical shape: to this aim, hollow cylindrical supports in polylactic acid (PLA) were designed and developed with a 3D printer (UPBOX Tiertime) (Fig. S2 in *Supplementary material*).

Intensive effort on the system miniaturization and optimization was dedicated to combine minimized polymer consumption and high level of accuracy of the rheological measurements (Paragraph S3 and Table S1 in *Supplementary material*). Based on these preliminary observations, the geometry of the hollow cylindrical supports was fixed to 7 mm of height and diameter ($h/d = 1$ mm/mm): a polymer saving of about 33 % (by weight) was obtained compared to studies in literature reporting similar hydrogels [20] and the reproducibility of the tests were ensured by intensive dedicated preliminary studies (results not shown).

Oscillatory shear experiments required a quite different geometry compared to compression studies: in this case, taking advantage of specific supports with a disk-like geometry, hydrogel disks of about 20 mm of diameter and 1.5 mm of thickness were used to ensure high-accuracy measurements (and low polymer consumption).

Using Ca^{2+} as ionic cross-linker (typically applied to study sEPS-based hydrogels [20,37]), various gelling conditions were tested for both AGS-extracted sEPS and model polymers (i.e., alginate and κ-/ι-carrageenan): polymer concentration = 1, 2.5, 5, 8 and 10 wt%; Ca^{2+} concentration = 0.001, 0.01, 0.05, 0.1, 0.5 and 1 M. Conceptual

phase diagrams were hence obtained, thus allowing the identification of the minimum polymer and Ca^{2+} concentrations needed for the hydrogel-formation. Furthermore, hydrogels were formed varying the type of metal cation M^{2+} used as ionic cross-linker: $M^{2+} = Ca^{2+}$, Cu^{2+}, Mg^{2+}, and Ni^{2+}. For more details, refer to Table S2 in *Supplementary material*.

To address the potential gelling behaviour of mixed protein–polysaccharide systems like sEPS, composite BSA (Bovine Serum Albumin)–alginate hydrogels (1 wt% alginate + 1 wt% BSA, 1 g BSA/g Alginate) were prepared in presence of 0.1 M Ca^{2+} and studied in comparison with pure alginate hydrogels (1 wt% alginate).

2.4. Post-gelling mechanical characterization

Various rheological measurements were combined to gain insights on the mechanics of the studied biopolymer-based systems. The robustness of the developed methodologies and the reproducibility of the obtained results were ensured by intensive dedicated studies performed in a wide range of operative conditions.

Biopolymer-based hydrogels formed by varying the sEPS concentration and (ionic) cross-linker concentration and nature (Table S2 in *Supplementary material*) were studied under (uniaxial) compression conditions. The hydrogels cylinders were subjected to consecutive compression–decompressions cycles (fixed compression–decompression duration: 2 + 2 min each), increasing the maximum deformation achieved in the loading step from 4 to 20 %. These mechanical tests were performed with a strain-controlled rheometer (Mars III, Thermo Scientific), using a parallel-plate geometry at room temperature (Fig. S3 in *Supplementary material*). All these experiments were carried out in a closed chamber at a controlled temperature (20 °C): the water loss of the studied hydrogels due to the moisture evaporation was hence assumed as negligible, especially considering the short time of the test (≃1 h). Load and displacement data, represented by normal force F_n [Pa] and deformed height of the sample h [mm], were collected during the experiments and the resulting stress σ [Pa] and deformation ε [%] were calculated according to the following equations (Eqs. 1 and 2):

$$\sigma = \frac{F_n}{\pi \cdot r^2} \tag{1}$$

$$\varepsilon = \frac{h_0 - h}{h_0} \cdot 100 \tag{2}$$

where h_0 and h [mm] are the original and deformed height of the hydrogel cylinder, respectively, while $\pi \bullet r^2$ [mm^2] is its cross-section area (in which r [mm] is the sample radius).

True stress σ_{true} [Pa] and compression parameter λ [–] were also calculated as follows (Eqs. 3 and 4):

$$\sigma_{true} = \frac{F_n}{\pi \cdot r^2} \cdot \lambda \tag{3}$$

$$\lambda = \frac{h}{h_0} \tag{4}$$

With respect to stress σ, true stress σ_{true} allowed normalizing data for the slight differences in terms of initial height of the samples over consecutive compression-decompression cycles. For convenience, stress was defined positive. The effect of the biaxial extension of the sample in the plane normal to the loading direction was assumed as negligible, as observed in preliminary studies (data not shown). The hysteresis (Pa = J/m^3), representing the energy dissipated during a loading-unloading cycle, was calculated approximating the area enclosed in the hysteresis loop (i.e., between loading and unloading curves, respectively) with the trapezoidal rule as described in *Supplementary material* (Fig. S4).

For each tested condition, the Young's modulus (E, kPa) was obtained from the linear regression of the σ–ε data in the linear elasticity domain of the material (in which the Hooke's law is objected, i.e., $\sigma = E \bullet \varepsilon$). For each loading-unloading cycle in the elastic region, a value of E was obtained and an average value for each sample was calculated as the mean on all the applied compression–decompression cycles in the linear elasticity domain. The elastic region for the E calculation was assumed to be the range of deformations over the consecutive compression-decompression cycles for which the σ–ε relation was kept linear (i.e., sample was able to recover the original state upon reduction of the mechanical load at a certain decompression rate). In other words, deformations recoverable in 2 min upon reduction of the mechanical load were assumed as elastic. These experiments were carried out in triplicate and the resulting Young's modulus was expressed as average value ± standard deviation among the tested samples (n. 3 hydrogels formed under the same gelling conditions).

A preliminary assessment of the long-term mechanical performance was implemented measuring the Young's modulus of 2.5 wt% alginate hydrogels (formed in presence of 0.1 M Ca^{2+}) over time. To this aim, after 24 h of dialysis against the Ca^{2+} aqueous solution, the hydrogel was collected from the cylindrical support, transferred into the ionic cross-linker aqueous solution and stored at 4 °C before being subjected to mechanical test at pre-selected time intervals. Because of the significant reduction of the hydrogel stiffness observed over time (≃47.5 ± 3.4, 39.7 ± 1.0, 27.4 ± 3.0 kPa after 1, 3 and 6 days of storage, respectively), all the experiments were carried out after 1 day storage (4 °C) in the corresponding ionic cross-linker aqueous solution.

To gather further insights on their mechanical behaviour, sEPS-based systems with increasing polymer concentrations (1–10 wt% sEPS) obtained in presence of 0.5 M Ca^{2+} were also subjected to oscillatory shear measurements. Since the mechanical similarities between the studied sEPS, only the results related to $sEPS_B$ are reported. These experiments were performed by using a plate-plate geometry (20 mm diameter, 400 μm gap) on a Discovery Hybrid Rheometer (Disc.HR-3, TA Instruments) working in controlled shear stress mode. The frequency dependence of the storage modulus G' and loss modulus G'' was investigated through frequency sweep test in the frequency range 0.01–100 Hz (strain amplitude γ = 0.4 %). All the measurements were carried out in the Linear Viscoelastic region of deformations (LVE) previously determined for each sample by means of amplitude sweep test (the amplitude of the imposed strain varied between 0.01 and 40 % with a constant frequency of 1 Hz).

All these experiments were performed at a constant temperature of 25.00 ± 0.01 °C. The complex viscosity ($|\eta^*|$) was calculated as follows (Eq. 5):

$$|\eta^*| = \sqrt{\frac{G'^2(\omega) + G''^2(\omega)}{\omega^2}} \tag{5}$$

More details on the theory of the described oscillatory shear experiments are given in *Appendix* (Paragraph S5).

3. Results and discussion

3.1. Hydrogel-formation of sEPS versus model biopolymers

The distinct biopolymer nature resulted in a different response to various hydrogel-forming conditions. Particularly, the hydrogel-formation appeared differently influenced by polymer concentration and (ionic) cross-linker concentration and nature. The effect of polymer and (ionic) cross-linker concentrations was addressed for biopolymer-based hydrogels formed in presence of Ca^{2+}. In this regard, Fig. 1 illustrates the conceptual phase diagrams related to $sEPS_A$, $sEPS_B$ and alginate covering the range of 1–10 wt% polymer concentration and 0.001–1 M Ca^{2+} concentration. Regardless of the origin of the microbial aggregate (i.e., AGS from R_A and R_B), sEPS were able to form stable and stiff hydrogels at concentrations higher than 2.5 wt% in presence of high calcium contents (at least 0.1 M) (Fig. 1a and b). To be noticed that at 2.5 wt%, hydrogels obtained with $sEPS_B$ were not sufficiently stiff to be tested via rheometry under compression conditions regardless of the

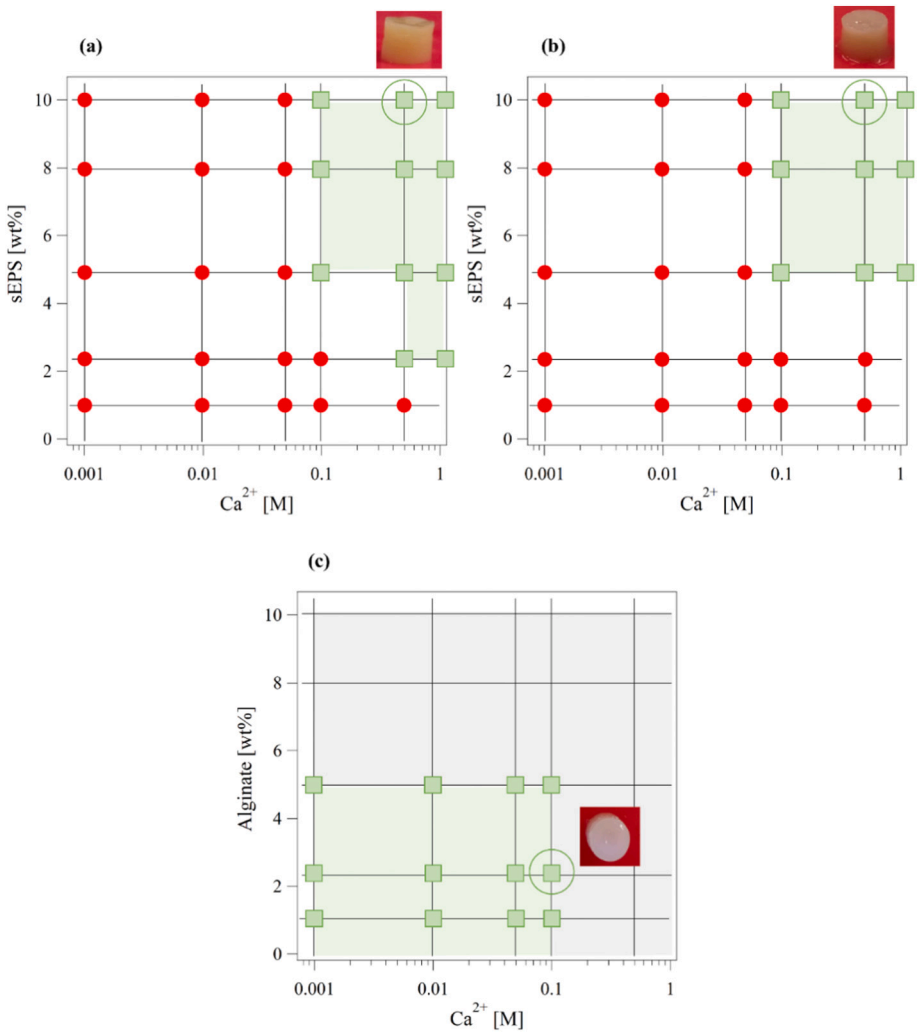

Fig. 1. Conceptual phase diagrams of $sEPS_A$ (a), $sEPS_B$ (b) and alginate (c) hydrogels (1–10 wt% polymer concentrations) formed in presence of increasing Ca^{2+} concentrations (0.001–1 M). X-axis is expressed in log scale. The red markers represent the polymer–Ca^{2+} concentrations for which the hydrogel-formation was not observed (or the obtained hydrogel-like materials were not sufficiently stiff to be tested via rheometry under compression conditions). The green markers defined the region in terms polymer–Ca^{2+} concentrations allowing the established of an extended 3D network (and hence stable and stiff hydrogels). In panel c, the conditions in the grey area ($[Ca^{2+}] \geq 0.1$ M; [Alginate] ≥ 5 wt%) were not tested for alginate. (For interpretation of the references to colour in this figure legend, the reader is referred to the web version of this article.)

Ca^{2+} concentration.

The comparison with model biopolymers (i.e., alginate and κ-/ι-carrageenan) disclosed that the sEPS hydrogel-formation was allowed by higher driving forces (e.g., Ca^{2+} concentrations) and polymer concentrations. Indeed, alginate was able to form stable hydrogels under all the tested conditions ($[Ca^{2+}] \geq 0.001$ M; [Alginate] ≥ 1 wt%, Fig. 1c). The κ-/ι-carrageenan hydrogel-formation occurred for all the tested range of polymer concentrations ([κ-/ι-carrageenan] ≥ 1 wt%) and did not appear strictly dependent on the Ca^{2+} concentration adopted (for this reason their conceptual phase diagrams were not reported in Fig. 1): in fact, κ-/ι-carrageenan dispersions underwent sol-gel transition upon cooling without adding (external) divalent metal ions (i.e., $[Ca^{2+}] = 0$ M). The presence of Na^+ ions in the pristine aqueous dispersions (stable at high temperatures, $T \geq 65$ °C) which are able to ionically bound to sulphate groups of the carrageenan units might favor polymer aggregation and therefore gelation upon cooling [42].

All the studied biopolymers (i.e., sEPS, alginate, and κ-/ι-carrageenan) were able to form hydrogels in presence of divalent metal cations M^{2+}. Hydrogels are gels able to reversibly sorb and exude water and/or biological fluids (i.e., swell, and de-swell) [5]. Swelling requires the existence of hydrophilic groups within the polymeric network, which is a condition common to all the studied biopolymers. The ability to form hydrogels via ionic cross-linking was instead driven by the abundance of (acidic) functionals groups (e.g., carboxyl and sulphate-half ester groups for alginate and κ-/ι-carrageenan, respectively) able to interact with metal cations during the cross-linking reaction, thus leading to the formation of an extended 3D network. As widely reported in literature [18,25] and confirmed by FT-IR spectroscopy in this study (Fig. S7 in *Supplementary material*), AGS-extracted sEPS contain various functional groups (e.g., carboxyl, hydroxyl, amino groups, etc.) representing potential metal-binding sites involved in the hydrogel-formation processes. As arisen from literature data [18,25], chemical and functional similarities between sodium alginate and sEPS from AGS treating municipal sewage could be found looking at the results emerging from the FT-IR spectroscopy characterization; however, AGS-derived sEPS have been demonstrated much more complex with respect to pure alginate [20]. More significative chemical differences might be found between sEPS and κ-/ι-carrageenan. Indeed, κ-/ι-carrageenan present FT-IR spectra typical of sulphonated polysaccharides from red seaweeds with the characteristic broad band of sulphate esters (S=O) between 1210 and 1260 cm^{-1} and the strong ones at 930 cm^{-1} assigned to 3,6-anhydro-galactose residues [46]. These qualitative observations preliminarily indicated the high-diversity and complexity characterizing the sEPS matrix: with respect to the studied model biopolymers, AGS-extracted sEPS might contain compounds not effectively participating in the gelling processes, thus making the cross-linking effectiveness dependent on higher driving forces (e.g., Ca^{2+} concentrations) and polymer concentrations. The dependence of the hydrogel mechanics on the applied gelling conditions (e.g., polymer concentration and ionic cross-linker concentration and nature) has been confirmed and discussed with more details based on the results emerged from the rheological characterization (under both compression and

shear stress conditions), as described in the following paragraphs.

3.2. Compression studies

3.2.1. Stress-strain response to consecutive compression-decompression cycles

The stress-strain response to consecutive compression-decompression cycles disclosed mechanical differences among the tested biopolymer-based hydrogels. However, the overall mechanical behaviour seemed to be preserved over the wide range of hydrogel-forming conditions applied (i.e., polymer concentration and ionic cross-linker concentration and nature). By way of example, Fig. 2 plots the true stress σ_{true} against the compression parameter λ over the consecutive loading–unloading cycles applied on 5 wt% alginate, κ-/ι-carrageenan and sEPS hydrogels formed in presence of 0.1 M Ca^{2+}. Regardless of the origin of the microbial aggregates (i.e., AGS from R_A and R_B), sEPS hydrogels deformed elastically for all the applied range of deformations (up to 20 %) over the consecutive compression–decompression cycles, as confirmed by the linearity and overlapping of loading curves (Fig. 2a). Even if characterized by significative differences in terms of hydrogel-forming mechanisms and biochemical composition, ι-carrageenan hydrogels behaved similarly to sEPS hydrogels (Fig. 2b). Conversely, for κ-carrageenan and alginate hydrogels the linear elastic behaviour seemed to be maintained over the first loading–unloading cycles up to a maximum deformation $\varepsilon = 10$–15 % (Fig. 2c, d): above this threshold, the σ_{true}–λ plots exhibited a stress plateau followed by a section with a higher slope, thus suggesting the occurrence of many non-reversible deformations in the cross-linked polymeric network. In this case, the decompression rate might be not slow enough to equilibrate the stresses in the hydrogel structure, leaving a residual deformation not recoverable at the end of the unloading phase [47].

Moreover, for alginate and κ-carrageenan hydrogels the loading and unloading curves did not match. This type of behaviour, referred to hysteresis, is common in viscoelastic materials and it is the result of energy dissipation, fluid diffusion and polymer molecular realignment during loading [48]. The hysteresis, and therefore the energy dissipated during a loading–unloading cycle, increased as a function of the maximum deformation achieved in the loading step over the consecutive compression–decompression cycles but also upon increasing the polymer concentration (Fig. S8 in *Supplementary material*).

The observed mechanical profiles could be interpreted looking at the hydrogel structure (Fig. S9 in *Supplementary material*). A hydrogel consists of a network of polymeric chains swollen in aqueous solution: the network endows the elastic and plastic features while the aqueous phase provides the viscous properties. Water in the hydrogel might be classified as bound and free water. Free water does not interact with the polymeric chains, and it is assumed to fill the space within the network: consequently, it is able to be redistributed when the hydrogel is deformed. When a strain is applied to the hydrogel (e.g., the hydrogel is compressed), fluid is pushed through the pores in the polymeric network and the polymer chains are realigned. As the strain is increased, the ability of fluid to pass through pores is reduced and the polymer chains stiffen [48], thus increasing the energy dissipation and therefore the

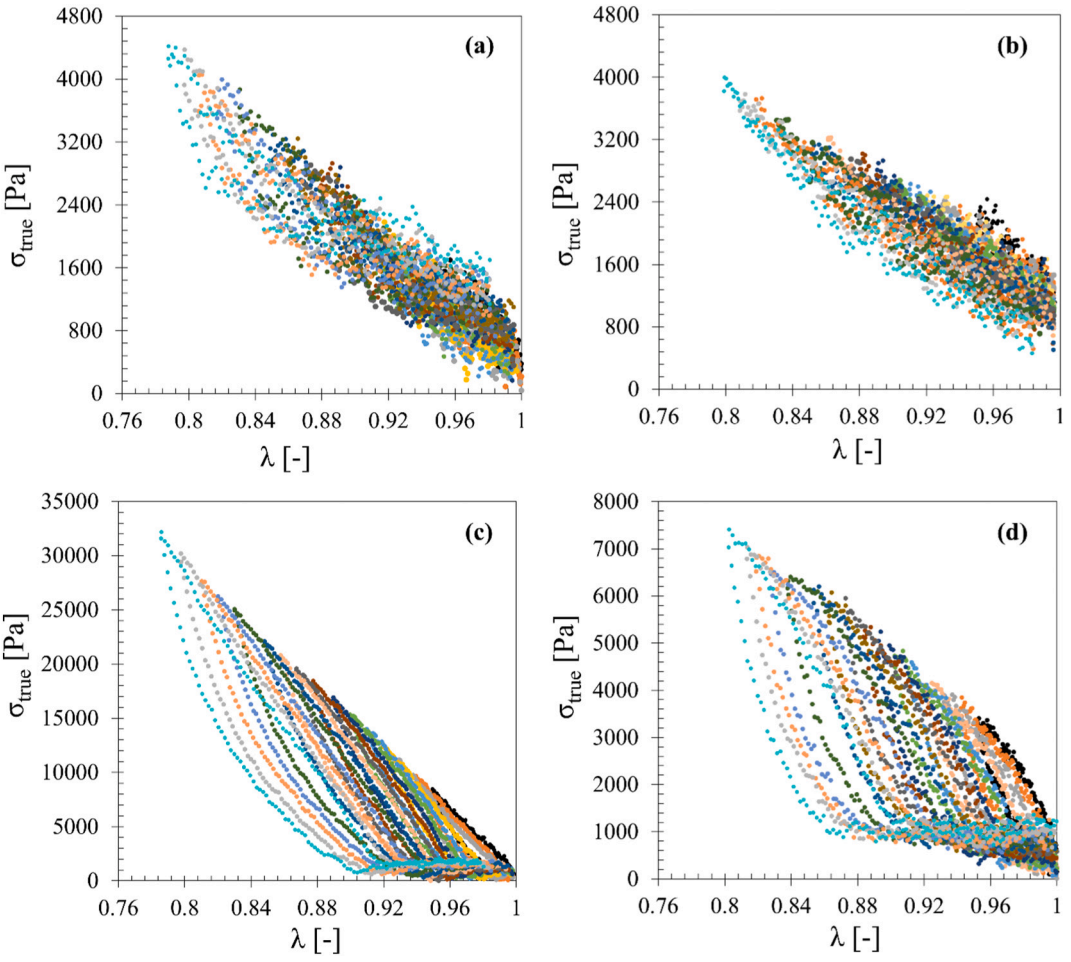

Fig. 2. Stress-strain plots related to consecutive compression–decompression cycles on 5 % (w/v) $sEPS_A$ (a), ι-carrageenan (b), κ-carrageenan (c), and alginate (d) hydrogels obtained in presence of 0.1 M Ca^{2+} as ionic cross-linker. Each loading–unloading cycle is represented in a different colour.

hysteresis. The same behaviour might be evidenced upon increasing the polymer concentration (i.e., the cross-linking density) which might decrease the network porosity. With respect to alginate and κ-carrageenan, sEPS and ι-carrageenan hydrogels featured more significative linear elastic properties for a broader range of deformations (i.e., they were able to recover the deformation upon reduction of the mechanical load): this behaviour could be influenced by the greater ability of (free) water to be redistributed in the space within the network upon compression.

3.2.2. *Effect of the gelling conditions on the hydrogel stiffness*

The Young's modulus *E* (and therefore the hydrogel stiffness) appeared significantly affected by polymer concentration and (ionic) cross-linker concentration and nature, thus proving to be an eligible parameter to give insights on the hydrogel-formation processes and resulting post-gelling mechanical properties.

3.2.2.1. Effect of polymer concentration and composition. Regardless of the distinct hydrogel-forming mechanism and biopolymer nature, the Young's moduli *E* increased linearly with the polymer concentration in the tested range (Fig. 3) likely due to the increasing polymer chain density and entanglement [36]. Depending on the origin of the microbial aggregate (i.e., AGS from R_A and R_B), sEPS hydrogels formed in presence of 1 M Ca^{2+} evidenced different stiffness at the same polymer concentration (wt% sEPS): indeed, *E* increased from about 2.9 to 15.7 kPa upon increasing the polymer concentration from 2.5 to 10 wt% for $sEPS_A$ hydrogels, while $sEPS_B$ presented lower levels of post-gelling stiffness in all the investigated range of polymer concentrations. Moreover, the *E* values were significantly different among the tested biopolymers: for example, at 5 wt% polymer concentration, κ-carrageenan was able to form the stiffest hydrogels (168.8 ± 10.8 kPa) in presence of Ca^{2+} as ionic cross-linker, followed by alginate (60.0 ± 0.6 kPa), ι-carrageenan (19.5 ± 2.2 kPa), and sEPS (6.2 ± 0.7 kPa for $sEPS_A$ and 3.9 ± 0.2 kPa for $sEPS_B$). The differences in terms of post-gelling stiffness can be ascribed to the structural and compositional features of the investigated polymers. κ-Carrageenan and ι-carrageenan contains one and two sulphate groups, respectively, for each elemental unit of the polymer chain. Sulphates are negatively charged groups with a big steric

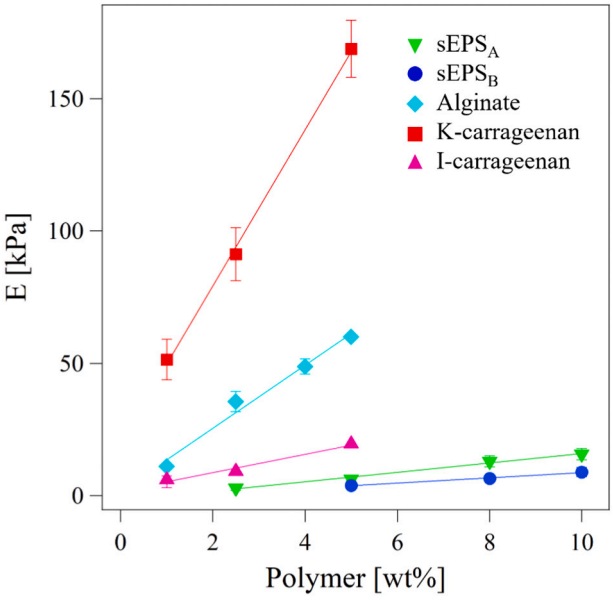

Fig. 3. Effect of polymer concentration on κ-/ι-carrageenan, alginate, and sEPS post-gelling stiffness. [Ca^{2+}] = 0.1 and 1 M for model biopolymers and sEPS, respectively. Data = average value ± standard deviation (n. 3 sample replications).

hindrance: the higher number of sulphate residues in the ι-carrageenan macromolecules, that are bulky and repulse each other electrostatically, can hinder the formation of double or single helixes and inhibit their subsequent aggregation, thus leading to weaker hydrogels compared to κ-carrageenan [49]. The high guluronic acid content of alginate resulted in the formation of stiff hydrogels due to cross-linking of G-blocks [20]. Alginate interacts with Ca^{2+} ions via its carboxyl groups that are distributed on a linear polysaccharidic chain: the abundance and accessibility of metal-binding sites might therefore result in stiff hydrogels (even at relatively low polymer concentrations).

The high-complexity and diversity of the extracellular biopolymeric matrix might be at the basis of the lower mechanical performance observed in comparison with the studied model biopolymers. Indeed, sEPS are a complex mixture of proteins, neutral sugars, amino sugars, uronic acids and humic compounds: they are hence characterized by a much higher diversity of sugar monomers with respect to alginate [50]. It is therefore not surprisingly that cross-linking reactions occurring via Ca^{2+} complexation with carboxyl groups resulted in weaker hydrogels for sEPS than for alginate [20]. Additionally, sulphate groups in EPS [51] could have a role in the hydrogel-formation: they could interact with M^{2+} ions during the gelling processes, thus acting as potential metal-binding sites; on the other side, an excessive sulphate content could hinder the polymer chain cross-linking, similarly to what described for the ι-carrageenan macromolecules.

Furthermore, it is reasonable to speculate that not all the sEPS components are directly involved in the hydrogel-formation. The exact fraction of hydrogel-forming macromolecules in the sEPS extracts would hence appear unknown and the concentration of gelling sEPS may be overestimated. There is no consensus in literature about the role of polysaccharides and proteins in the gelling properties of microbial aggregates [37]. Proteins should have an important role in bonding EPS due to their high affinity for cations [52]. Although the protein hydrophobicity is believed to be helpful for the gel-formation [53], some studies consider polysaccharides or types of glycosides (e.g., proteoglycans) as key macromolecules responsible for the EPS gelling ability, observing post-gelling mechanical properties independent from the protein content [54]. Schambeck et al. [37] reported that peptide and peptidoglycans bonds may not play a role on gel-forming properties of sEPS, while uronic carbohydrates containing mannuronic acids are key molecules involved in the sEPS gel-formation and hydrogel cohesion. In this study, indirect observations based on composite alginate–BSA hydrogels agreed these evidences. Alginate and alginate–BSA composite hydrogels presented similar Young's moduli ($E = 14.4 \pm 0.6$ kPa versus 13.9 ± 1.1 kPa, respectively), thus proving the negligible influence of BSA on the alginate post-gelling stiffness. Even if the sEPS biochemical composition is much more complex and diverse, this preliminary result suggested that the sEPS post-gelling stiffness could be more strongly associated to the content of polysaccharide-like substances. Further investigations are encouraged to shed light on these aspects: particularly, a key point which remains to be clarified is the level of purity of the extractable sEPS macromolecules in order to avoid a potential overestimation of the effective sEPS gelling compounds. Interestingly, the higher content of uronic acids of $sEPS_B$ with respect to $sEPS_A$ (Fig. S1 in *Supplementary material*) did not result in stiffer hydrogels: even if uronic sugars are considered strongly involved in the hydrogel cohesion, it is not only their content, but also their type that govern the sEPS hydrogel elasticity [37]. Particularly, mannuronic acids form weaker hydrogels [55] and have been suggested to be present in higher contents in sEPS extracted from AGS fed with VFA-rich wastewaters (i.e., simple synthetic influents) [37].

The lower *E* values observed for both $sEPS_A$ and $sEPS_B$ with respect to the model biopolymers can be also due to the lower spatial density of the available binding sites that could be partially occupied by the divalent metal cations intrinsically present into the extracted sEPS (i.e., adsorbed from the treated wastewater by sEPS into the pristine biomass).

Overall, for all the tested biopolymer-based hydrogels, the observed

Young's moduli appeared significantly lowered compared to traditional engineering materials and/or synthetic polymers likely due to the high-water content (ranging between 90 and 97.5 % wt). Indeed, as previously explained, the elastic/plastic properties of hydrogel-like systems are given by the polymeric network, while the aqueous phase provides the viscous features that do not significantly contribute to the post-gelling stiffness.

3.2.2.2. Effect of (ionic) cross-linker concentration. As previously introduced, stable sEPS hydrogels (i.e. with measurable mechanical properties under compression) were not obtained in presence of Ca^{2+} concentration lower than 0.1 M, even increasing the sEPS content up to 10 wt%; conversely, alginate was able to undergo sol-gel transition for all the studied range of (ionic) cross-linker concentrations (0.001–0.1 M Ca^{2+}). The dependence of the post-gelling stiffness on the applied driving force was therefore established and studied in terms of E–Ca^{2+} concentration relationship both for alginate and sEPS. The effect of the cross-linker content on the κ-/ι-carrageenan post-gelling mechanics were not assessed: their ability to undergo sol-gel transition without addition of divalent metal cation makes this dependence less significative compared to the other studied biopolymer-based systems.

Fig. 4 shows the Young's moduli of sEPS and alginate hydrogels obtained in presence of increasing concentrations of Ca^{2+} as cross-linker. The post-gelling stiffness increased upon increasing Ca^{2+} concentration up to a threshold limit, above which different post-gelling mechanical responses were observed among the tested biopolymers. Increasing Ca^{2+} concentrations could likely promote higher cross-linking densities, thus leading to increasing E values [36]. Moreover, higher Ca^{2+} concentrations in the cross-linker solution would result in higher gradients between the core of the biopolymer-based system and the outside aqueous medium, thus favouring the Ca^{2+} ion diffusion into the polymeric matrix and hence formation of an extended 3D network. The effect of an increased Ca^{2+} concentration was negligible above 0.05 M and 0.5 M for alginate and $sEPS_A$ hydrogels, respectively, corresponding to 0.37 mol Ca/g Alginate and 1.16 mol Ca/g sEPS, which means that the saturation of the available Ca^{2+}-binding sites was probably achieved under these conditions. Conversely, while for the lowest Ca^{2+} concentrations $sEPS_A$ and $sEPS_B$ presented comparable post-gelling stiffness, at 1 M Ca^{2+} concentration the Young's modulus of

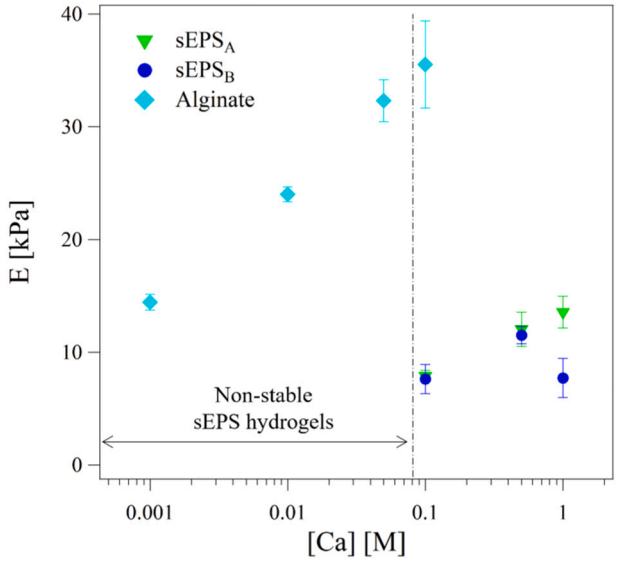

Fig. 4. Effect of Ca^{2+} concentration (as ionic cross-linker) on the sEPS and alginate post-gelling stiffness. The polymer concentrations were the following: [sEPS] = 8 wt%; [Alginate] = 2.5 wt%. X-axis is represented in log-scale for a clearer visualization. Data = average value ± standard deviation (n. 3 sample replications).

$sEPS_B$ hydrogels appeared 40–50 % lower compared to that of $sEPS_A$ hydrogels: this might be due to the formation of precipitates within the polymers (e.g., $NaCO_3$ and/or $CaCO_3$) favoured by the stronger alkaline conditions of the original $sEPS_B$ dispersions (pH ≃ 10.5–11.5), which could form a layer on the polymer surface hindering the (ionic) cross-linker diffusion inside the sEPS matrix. Particularly, $Ca(OH)_2$ precipitation was observed for pH between 8 and 12 and it increased linearly with the pH value (data not shown). The evaluation of the Ca^{2+} concentration as driving force is hence dependent on the pH and resulting presence of insoluble $Ca(OH)_2$. Considering the distinct pH conditions of the pristine sEPS dispersions, the Ca^{2+} diffusion as well as the initial amount of $Ca(OH)_2$ (part of which could be solubilized during dialysis) are expected to be different. Another potential explanation is that an excessive calcium concentration (>0.5 M in the case of $sEPS_B$ and in general depending on the available Ca^{2+}-binding sites) might promote too fast ion diffusion kinetics thus resulting in inhomogeneous cross-linking processes, which decreases the post-gelling stiffness and elasticity. Indeed, with reference to alginate, it has been found that high Ca^{2+} concentrations promote the formation of mono-complexes and egg-box dimers, generating a dense and elastic hydrogel structure with increased strength and stiffness. However, excessive Ca^{2+} concentrations could lead to heterogeneous binding with alginate and thus inhibit the formation of complete-symmetrical egg-box dimers, promoting the cross-linking between and within the alginate molecules [56,57]. Moreover, excessive Ca^{2+} could produce the collapse of gel network by crosslinking with MG blocks, which decreases the gel thermodynamic stability [58].

Overall, as noticeable in Fig. 4, the minimum Ca^{2+} concentration needed to obtain stiff hydrogels was higher for sEPS than alginate. This could result from the dilution of the effective sEPS hydrogel-forming macromolecules due to the presence of non-gelling compounds in the sEPS extracts.

3.2.2.3. Effect of (ionic) cross-linker nature. The hydrogel stiffness was significantly affected by the metal cation M^{2+} used as (ionic) cross-linker (e.g., Mg^{2+}, Ni^{2+}, Ca^{2+}, Cu^{2+}), as summarized in Fig. 5. Particularly, the alginate post-gelling stiffness increased in the following order: $Ni^{2+} \ll Ca^{2+} < Cu^{2+}$ (Fig. 5a), but alginate was not able to form stable hydrogels in presence of Mg^{2+}. Literature generally reports that alginate gelation via Mg^{2+}-driven cross-linking does not occur due to the lack of strong polymer–ion interactions; in addition, many researchers described Mg^{2+} ions as diffusively bound, if compared to strongly site-bounded ions like Ca^{2+} [59]. Despite the origin of the microbial aggregates (AGS from R_A and R_B) and resulting differences in terms of biochemical composition, $sEPS_A$ and $sEPS_B$ featured comparable selectivity in interacting with divalent metal cations during the cross-linking reaction ($Mg^{2+} < Ca^{2+} \sim Ni^{2+} < Cu^{2+}$, Fig. 5a), thus resulting in hydrogels with similar Young's moduli, with the exception of Mg^{2+}. Indeed, $sEPS_B$ were not able to form stable hydrogels in presence of Mg^{2+}, similarly to what observed for alginate. Both alginate and sEPS formed the stiffest hydrogels in presence of Cu^{2+}. However, the copper cross-linked hydrogels appeared inhomogeneous likely due to the high polymer affinity for complex formation with this metal [20,38,60]. Moreover, too fast gelation kinetic driven by the high polymer affinity for Cu^{2+} could result in inhomogeneous structures and hence in compromised post-gelling mechanical features.

Comparing alginate and sEPS to κ-/ι-carrageenan hydrogels, more significative differences were pointed out as a result of the distinct functional groups and mechanisms involved in the hydrogel-formation. As previously explained, κ-/ι-carrageenan dispersions (in 0.01 M NaOH) can undergo sol-gel transition upon cooling without addition of external divalent ions. However, the post-gelling stiffness was improved by adding external divalent metal ions in the following order (Fig. 5b): $Ca^{2+} < Cu^{2+} < Mg^{2+} \sim Ni^{2+}$ for κ-carrageenan and $Ca^{2+} \sim Mg^{2+} < Cu^{2+} < Ni^{2+}$ for ι-carrageenan. Indeed, small monovalent ions like Na^{+}

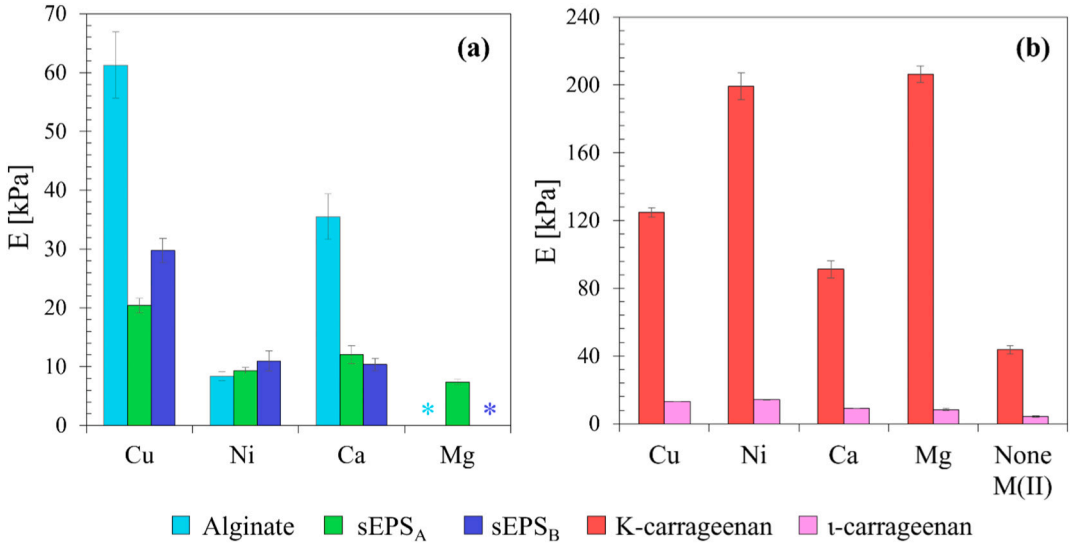

Fig. 5. Effect of various divalent metal cations as (ionic) cross-linker on the post-gelling stiffness of alginate, sEPS (a) and κ-/ι-carrageenan (b). The polymer and ionic cross-linker concentrations were the following: [M^{2+}] = 0.1 and 0.5 M, for model biopolymers and sEPS, respectively. [Model biopolymers] = 2.5 wt%; [sEPS] = 8 wt%. Data = average value ± standard deviation (n. 3 sample replications).

are only able to bond ionically to the sulphate groups reducing their efficacy in controlling the flexibility of disaccharide units of carrageenan. Conversely, divalent cations are able to form intra-molecular bridges between the sulphate groups of adjacent anhydro-D-galactose and D-galactose residues of carrageenan; upon cooling, the quaternary structure forms due to intermolecular M^{2+} bridging [42].

The hydrogel mechanics is influenced by the polymer affinity towards M^{2+} which in turn is affected by type and availability of binding sites and polymer conformation (i.e., polymeric chain arrangement) [20]. In this regard, the comparison between sEPS and alginate, characterized by more significative similarities compared to κ-/ι-carrageenan, was highlighted. As above-mentioned, the metal-binding ability is enabled by the abundance of acidic functional groups (e.g., carboxyl, amino, hydroxyl and phosphate groups [28,29]) and hence by the presence of various organic fractions (e.g., proteins, humic compounds, sugars, uronic acids, etc.) able to interact with M^{2+} ions with varying degrees of specificity and affinity. With respect to alginate, the much more complex 3D structure as well as the high-diversity of the sEPS matrix could suggest the participation of multiple functional groups (and hence various and heterogeneous binding sites) during the cross-linking reaction, as already highlighted by Felz et al. [20]. Wei et al. [61] observed that the Cu^{2+}-binding ability of the various activated sludge-derived EPS components exhibit the following decreasing trend: proteins > polysaccharides > humic acids; conversely, humic acids were the most efficient in binding Zn^{2+} (followed by proteins and polysaccharides). Through FT-IR analyses, the same authors studied the functional groups involved in the M^{2+}-binding processes: (i) for the EPS-related proteins, the metal uptake was mainly ascribed amide I and amide II groups, (ii) EPS-derived polysaccharides bound M^{2+} through carbonyl C═O, aromatic C═C and aliphatic C—H groups, while (iii) carbonyl C═O and aromatic C═C stretching within the humic acid mainly contributed to the removal of M^{2+} from the bulk medium. Li et al. [62] observed that carboxyl groups of proteins have the fastest response in binding Cu^{2+}compared to polysaccharides and hydrocarbons in EPS from anammox granular sludge. Through a complete set of techniques, Sheng et al. [63] demonstrated that both proteins and humic substances in EPS are strong ligands for Cu^{2+}, indicating that the copper binds to the carboxyl groups of the EPS macromolecules through an exothermic and thermodynamically favourable reaction. Polysaccharides, proteins and humic-like substances of AGS-derived EPS have been reported to bind Ni^{2+}, with hydroxyl and amino groups as key functional groups involved [28]. The higher selectivity for Ni^{2+} extended by AGS-extracted sEPS during the cross-linking reaction with respect to alginate could be hence due to the relatively high content of proteinaceous and humic compounds (together accounting for about 69 and 46 wt% of the sEPS organic matter in sEPS$_A$ and sEPS$_B$, respectively; Fig. S1 in *Supplementary material*). Phosphate is another functional group potentially involved in the M^{2+}-EPS interactions (and hence in the AGS-derived sEPS gelling processes): particularly, the ability of amino acids and phosphates to bind with Mg^{2+} [20] could be at the basis of hydrogel-formation observed in presence of Mg^{2+} for sEPS$_A$ and not for sEPS$_B$ and alginate.

It has been reported that EPS extracted with chemical methods feature significant differences in terms of metal-binding ability, likely due to contamination of the recovered polymers with the chemicals used during the extraction phase [64]: for instance, the polymer contamination by ions (e.g., Na^+) competing with the cross-linker M^{2+} for the available active sites could compromise the sEPS hydrogel-forming performance. The extraction/recovery method could also affect the polymer chain arrangement and resulting binding site availability, thus influencing the sEPS-M^{2+} interaction.

To gather further information on the nature of the polymer-M^{2+} interaction, the correlation between hydrogel stiffness and chemical properties of the ionic cross-linker was addressed, pointing out some differences in the chemistry of the sEPS and alginate hydrogel-formation. Alginate favoured alkaline earth metals and Cu^{2+} to form stiffer hydrogels: the selectivity for alkaline earth metal ions is reported to be dependent on the M/G ratio in the alginate backbone, especially in terms of G-block content involved in the hydrogel-formation [38]. The alginate post-gelling stiffness was directly related to intrinsic chemical properties of the ionic cross-linker such as metal affinity (or logarithm of the association constant, LogK_{ass}) for alginate and ionic radius (Fig. S10a in *Supplementary material*) in agreement with literature data [60]. Values corresponding to Cu^{2+} did not respect these linear correlations, likely due to the heterogeneous structure of hydrogels formed in presence of Cu^{2+} [60]. Even if clear correlations between post-gelling stiffness and metal properties were not detected for sEPS, an overall preference for transition metals with increasing atomic number was highlighted (Fig. S10b in *Supplementary material*). Various compounds potentially present in the AGS-derived sEPS (e.g., multiple amino acids and polyphosphates) have been reported to favour transition over alkaline earth metals [20]. Overall, the trend observed in terms of M^{2+} selectivity

agreed literature data [20], thus suggesting that the sEPS hydrogel-formation could be driven by similar mechanisms and chemical functions regardless of the origin of the microbial aggregates. In the case of Mg^{2+}, the cross-linking effectiveness would appear more dependent on the sEPS compositional properties. Further investigations are thus needed to shed light on the impact of the AGS-based treatment process (e.g., physical-chemical features and microbial population of the pristine biomass, characteristics of the treated wastewater, operational strategies, sludge retention time, environmental conditions, etc.) on the compositional, gelling and rheological properties of the extractable sEPS.

Furthermore, additional work is encouraged to gather insights on the M^{2+} selectivity of the recoverable sEPS and its consequences on the properties of the resulting hydrogels. To this aim, Isothermal Titration Calorimetry (ITC) coupled to Excitation-Emission Matrix (EEM) fluorescence spectroscopy may offer a deeper and more comprehensive analysis of the thermodynamic characteristics of the sEPS-M^{2+} binding reaction. Additionally, other techniques might be employed to provide more useful information about the M^{2+} binding mechanisms, including X-ray absorption fine structure (XAFS), FT-IR spectroscopy, electron paramagnetic resonance (EPR), etc. To support the sEPS-metal interaction considerations, it might be useful to compare the metals present in the extracted sEPS (for which high affinity can be speculated) to those more effectively used as an ionic crosslinker during the formation of hydrogel. Indeed, as pointed out in a previous article [29], a large part of the metals initially present in the treated wastewater can be adsorbed by the EPS matrix in the biomass itself and are not solubilized during the extraction/recovery of the EPS. Thus, the content of various metals (e.g., Cu, Ni, Zn, etc.) of the sEPS itself is likely to give information on its M^{2+} affinity and selectivity. A complete set of rheological measurements (e.g., oscillatory shear experiments + compression studies) carried out by varying the M^{2+} and sEPS concentrations is recommended for each ionic cross-linker M^{2+} with the aim to: (i) identify the gelation point (and hence the minimum M^{2+} and sEPS concentrations needed for the formation of an extended 3D network) and (ii) elucidate the dependence of the post-gelling mechanical parameters on the applied hydrogel-forming conditions. For instance, the comparison of the conceptual phase diagrams (with the related rheological information) obtained varying the ionic cross-linker M^{2+} might be useful to give a comprehensive overview of the sEPS ability in a wider range of operative conditions.

3.3. Oscillatory shear measurements

Further mechanical insights on sEPS-based hydrogels have been inferred from the oscillatory shear measurements carried out by varying the sEPS concentration (1–10 wt% sEPS). For all the investigated sEPS-based systems the LVE-region was preliminarily determined through amplitude sweep tests (Fig. S11 in *Supplementary material*). These experiments showed that in the LVE-region G' and G'' appeared almost invariant (up to a γ value of about 1 %); moreover, G' resulted higher than G'' thus suggesting that all the samples behaved like viscoelastic solids. As the strain was increased, G' started to decrease, thus indicating the occurrence of a yield point (and therefore the end of the LVE-region) due to the structural breakdown of the polymeric network (i.e., non-linear behaviour). At higher strain, crossover of the G' and G'' profiles were observed: above this point (termed flow point), G'' exceeded G', thus evidencing a sample behaviour as liquid-like systems.

An amplitude strain $\gamma = 0.4$ % within the LVE-region was hence chosen for the frequency sweep (i.e., frequency-dependent) experiments. Fig. 6 illustrates the dependence of storage modulus G', loss modulus G'' and complex viscosity η^* on the oscillation frequency ω for all the investigated sEPS-based systems (from 1 to 10 wt% sEPS). The storage modulus G' appeared always larger than the loss modulus G'' and no crossover between the G' and G'' profiles was observed within the investigated range of frequencies. According to this trend, complex viscosity η^* decreased in all the studied range of frequencies. This

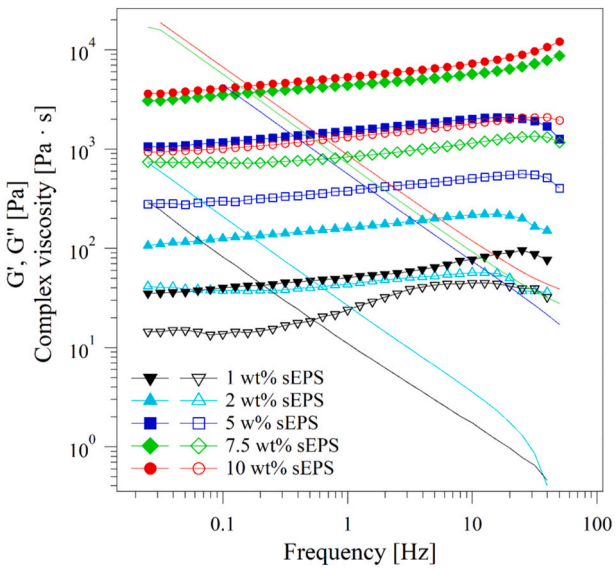

Fig. 6. Dependence of the storage modulus G' (full markers), loss modulus G'' (empty markers) and complex viscosity η^* (continuous lines) on the oscillation frequency for sEPS-based systems at increasing concentrations (1–10 wt % sEPS).

behaviour (i.e., $G' > G''$) is typical of systems presenting an infinite relaxation time τ. Being gels classified as fluids characterized by a solid-like behaviour (i.e., τ value that tends to infinite) [65], the trend observed suggested the gel-like nature of the studied sEPS-based systems. These results agreed with literature data: Schambeck et al. [37] reported for 2.3 wt% sEPS hydrogels from AGS fed with VFA-rich synthetic influents the same solid-like behaviour ($G' > G''$) with values of the storage modulus G' slightly lower compared to those observed in this study.

Furthermore, the storage modulus G' did not significantly depend on frequency (in the studied frequency range) but it appeared strictly affected by the sEPS concentration: G' values increased from about 50 Pa up to 5000 Pa upon increasing the sEPS concentration from 1 to 10 wt%, while the overall rheological behaviour remained almost the same, indicating that while the main relaxation mechanism was unchanged upon increasing the EPS concentration, the timescale of the process changed. As reported in literature, the storage modulus is proportional to the entanglement density ρ_E: $G' = \rho_E \bullet K_B \bullet T$, where K_B is the Boltzmann constant and T [K] is the temperature [66–68]: the increase of G' upon increasing the sEPS concentration in the studied sEPS-based hydrogel systems indicated an increase of ρ_E with the sEPS content, thus suggesting a higher complexity of the sample structure and an increased strength of the 3D network thus formed [68].

Further information on the hydrogel-formation might be speculated from the trend observed for the complex viscosity η^* upon variation of the sEPS concentrations (Fig. 7). The η^* values, extrapolated from the frequency sweep curves at an oscillation frequency $\omega = 1$ Hz, were approximately constant (in the order of 0.5–1 Pa·s) up to 2.5 wt% sEPS concentration and then significantly increased up to 870 Pa·s at 10 wt% sEPS concentration: this could indicate the presence of a concentration threshold between 2.5 and 5 wt% sEPS above which the formation of an extended 3D hydrogel network occurred. However, the mechanical profiles reported above evidenced a gel-like behaviour ($G' > G''$ in the LVE-region for all the applied range of oscillation frequencies) even at the lowest sEPS concentrations (<2.5 wt% sEPS). It can be hence speculated that for sEPS concentrations lower than 2.5 wt% only weakly interconnected polymeric clusters were present, while a strong increase in the cross-linking density, leading to the formation of an extended 3D network, can be observed upon increasing the sEPS above this concentration threshold.

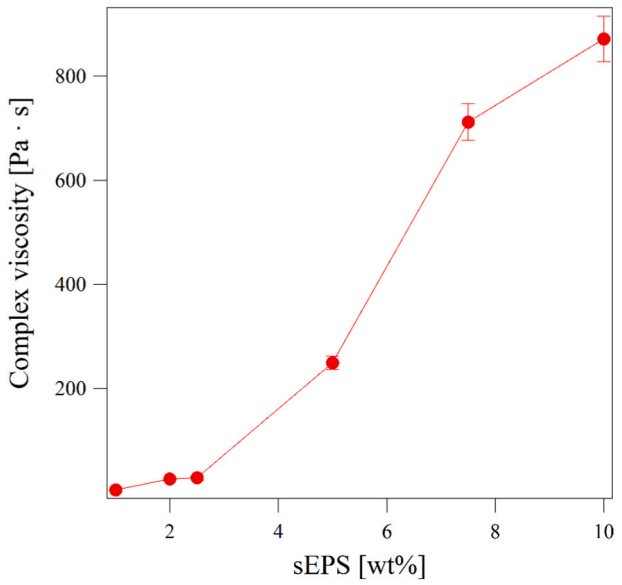

Fig. 7. Dependence of the viscosity η^* (at $\omega = 1$ Hz) on the sEPS concentration. The error bars represent the estimated error equal to 5 %.

Indeed, polymer cross-linking takes place if binding sites are available and if polymer chains can interact (which typically happens above a critical concentration) and it is strictly dependent on the nature of the macromolecules involved [5]. The cross-linking effectiveness would hence appear as a consequence of the weight (or volume) fraction of the gelling agent Φ. To this aim, the dependence of the storage modulus G' on Φ has been largely discussed in literature [68– 70]. In the present work, the G'–sEPS concentration relationship was established and satisfactorily described by a power-law function ($G' = a \bullet \Phi^n$ where $\Phi =$ wt% sEPS, $R^2 = 0.975$) (Fig. S12 in *Supplementary material*). The exponent value $n \simeq 2$ may be consistent with a site percolation process to describe the hydrogel-forming mechanisms. This model [71–73] is based on a critical phenomenon of connectivity. If p is the fraction of connected objects, a so-called percolation threshold p_c can be defined: below p_c only clusters are present, while above p_c an infinite network is formed [74]. If two neighboring sites are filled, a bond between them is established, thus producing clusters of size s with frequency n_s. The percolation threshold, p_c, can be therefore defined as the critical value of p at which the formation of a cluster occurs, which means that $s_{av} \rightarrow \infty$ where s_{av} represents the average cluster size (i.e., the number of sites forming the cluster itself) [75]. Interestingly, alginate gelation is generally described through a percolation model [76]: similar hydrogel-forming mechanisms might be hence promoted in presence of Ca^{2+} for AGS-derived sEPS and alginate, despite their chemical and functional differences.

3.4. Outlook and perspectives

The methodological constraints represent one of the main bottlenecks in matter of AGS-derived sEPS. To this aim, this paper tried to draw general guidelines to progress in this comprehensive research field: in line with the growing commercial interest in hydrogel-like materials, a dedicated focus on the study of the sEPS gelling ability was proposed. Selecting rheometry as eligible technique to shed light on the sEPS post-gelling mechanics, the hydrogel-forming methods have been optimized based on the following criteria (i) low polymer consumption, (ii) hydrogel homogeneity and (iii) accuracy of the rheometric measurements. Through a complete set of dedicated studies, the minimum hydrogel sizes allowing high-accuracy rheological measurements have been found (gel-like cylinders of about 7 mm in height and diameter for the compressions tests and gel-like disks of around 20 mm in diameter and 1.5 mm in height for the oscillatory shear measurements). This methodological finding could help to expand the bounders of the characterization studies, overcoming the obstacles due to the limited availability of adequate mass flows of AGS-derived sEPS from laboratory- and/or pilot-scale reactors. Moreover, the comparison with well-known biopolymers has proved to be a powerful tool to strengthen the outcome of rheology, especially considering the high-complexity and diversity of the treated matrices. However, future work is encouraged to shed light on the hydrogel structure and cross-linking processes through dedicated techniques (e.g., imaging techniques such as scanning electron microscopy SEM, transmission electron microscopy TEM and confocal laser scanning microscopy CLSM, Fourier Transform-InfraRed spectroscopy FT-IR, differential scanning calorimetry DSC, small-angle X-ray scattering SAXS, etc.), thus supporting the considerations proposed in this paper.

The results of the mechanical characterization indicated also appealing applicative potentials in the resource recovery framework. The dependence of the sEPS post-gelling mechanical properties (e.g., stiffness) on the applied hydrogel-forming conditions (e.g., polymer concentration and ionic cross-linker concentration and nature) could be exploited to develop waste-derived bioproducts to be valorized in multiple fields. AGS-derived sEPS can be used to form hydrogel-like materials with high-water content (up to 99 wt%) and solid-like mechanical behaviours: indeed, level of stiffness (E up to about 20 kPa under the tested conditions) comparable to other biopolymer-based systems currently applied for commercial purposes (e.g., ι-carrageenan hydrogels) could be achieved. The development of sEPS-based hydrogels with tunable mechanical features (e.g., stiffness, elasticity, viscosity) might cover a wide range of industrial solutions: if a higher stiffness is demanded, the mechanical features can be tailored by (i) controlling the cross-linking kinetics (e.g., via dialysis), (ii) increasing the ionic cross-linker M^{2+} and sEPS concentrations (i.e., higher cross-linking densities) and (iii) using M^{2+} with higher affinity (e.g., Cu^{2+}). Other strategies suggested in literature are (a) increasing the uronic sugar content (e.g., by enzymatic treatment) and (b) changing the length and proportion of guluronic and mannuronic blocks [37].

Even if a broader implementation might be limited in sectors related to direct human contact/consumption, a wide range of potential environment- and/or industry-related solutions common to other biopolymer-based systems (e.g., alginate, ι-carrageenan) could be explored.

The interesting rheological features of sEPS-based systems suggest their potential application as viscosity-modifying agents (VMAs): they could be studied as alternative to natural polymers (including microbial polysaccharides such as welan gum, diutan gum, and guar gum, cellulose, and starch) currently applied as VMAs in developing advanced cement-based materials with adapted rheology [77]. Appealing valorization scenarios might be also opened in the textile sector by replacing conventionally used thickener (mainly alginate) with AGS-derived sEPS. The main role of this thickener is to give the paste adequate rheological behaviour (e.g., good liquidity, thixotropy and viscoelastic properties), which significantly influence the final print quality [78]. To this aim, the sEPS concentration needed to achieve the desired viscosity should be identified (e.g., acquiring the flow curves though rheometry in rotational regime), eventually providing the addition of low concentrations of M^{2+} below the gelation threshold. Indeed, as emerged from the conceptual phase diagrams (Fig. 1) at qualitative level, low concentration of Ca^{2+} (<0.1 M) did not enable the establishment of an extended 3D network (which is not the desired for thickening applications) but enhanced the viscosity of the sEPS aqueous dispersions. The interactions among the sEPS-based thickeners, printing additives and dyes as well as the impact of all components on the rheological properties and printing performance of the past matrices should be then evaluated, thus exploring potential routes of more sustainable textile printing processes.

Thanks to their water-binding capacity, sEPS-based hydrogels might be also efficiently valorized in agriculture-related solutions. They could

be used for soil conditioning alternatively to poly(acrylic acid)/polyacrylamide-based materials that are non-renewable, contain potentially toxic monomers (e.g., acrylamide), and are biodegradable only to a limited extent [79]. Taking advantage of their rheological features, sEPS-based hydrogels might be also studied as vehicle systems for the slow-release of agrochemicals in soil (e.g., nutrients, phytostimulants, etc.). To progress towards sustainable agro-practices exploiting sEPS-derived biomaterials, the mechanical characterization should be combined with the investigation of many peculiar characteristics: (i) compositional properties (e.g., content of macro- and micro-nutrients, phytotoxic elements like heavy metals, etc.), (ii) ability to reversibly sorb and desorb water (i.e., swelling/de-swelling capacity), (iii) biodegradability and long-term stability under the natural soil conditions. In this interesting research field, the implementation of Differential Scanning Calorimetry (DSC) analyses to characterize the distinct free- and bound-water eventually after mechanical perturbation may be useful.

To progress towards a broader implementation of AGS-derived sEPS hydrogels in industry-related solutions, further research effort is expected to be dedicated on the assessment of the long-term mechanical performance: particularly, the maintenance of a solid-like mechanical behaviour over time might be fundamental in applications demanding mid- or long-term functionality of the developed biomaterials (e.g., slow-release of agrochemicals in soil).

As above-mentioned, the mechanical characterization cannot be sufficient to gain a comprehensive overview of the high potential of sEPS-based hydrogels as value-added biomaterials. A synergic approach able to integrate the assessment of multiple fundamental properties (e.g., mechanics, biochemical composition, physic-chemistry, biodegradability, etc.) should be drawn depending on the nature of the desired application area. An improvement of the industrial applicability of AGS-derived sEPS could change the critical status of waste sludge in WWTPs. In this perspective, the extraction/recovery procedures should be optimized according to application-related criteria: each treatment phase should be hence adapted (in terms of chemicals applied, chemical, physical and/or biological approaches implemented, etc.) depending on the specific requests of the targeted industrial application. For instance, this study demonstrated the feasibility to form sEPS hydrogels by means of different metal ions M^{2+} as cross-linker agent (e.g., Ca^{2+}, Ni^{2+}, Cu^{2+}, Mg^{2+}), thus resulting in various levels of stiffness and an almost unchanged overall mechanical behaviour (in terms of stress-strain response under compression). The choice of the ionic cross-linker should be therefore subordinated to the level of quality and mechanics demanded by the desired application field. Moreover, the ionic cross-linker source (i.e., the metal salt used to prepare the aqueous medium) should be carefully addressed. In this work, MCl_2 synthetic aqueous solutions were used as ionic cross-linker M^{2+} source: Cl^- ions could diffuse from the aqueous phase into the polymeric matrix together with M^{2+}, thus becoming part of the final hydrogel composition with potential limitations in environmental applications (e.g., agriculture). In this sense, the choice of adequate chemicals would be dependent on the standard imposed by the targeted application sector. Another key point to be addressed in implementing EPS-based biomaterials should concern the variability of the EPS characteristics (e.g., physical-chemical, compositional and rheological features) upon fluctuations of the AGS-based process (in terms of load, performance, environmental conditions due to the seasonality, etc.). These process variations could influence the quality/quantity of the extractable sEPS macromolecules and resulting properties, thus generating a potential constrain for their valorization in standardized industrial solutions. For instance, thickeners for textile printing imply targeted and constant compositions and mechanical properties and the feasibility of keeping them unchanged upon variations of the EPS production process conditions could be challenging. Conversely, lower constrains in terms of variability might be involved in agriculture-related applications (e.g., soil conditioners and/or as coating agents for fertilizing products to control the nutrient release kinetics). Furthermore, the integration of EPS recovery processes in WWTPs treating certain kinds of industrial influents characterized by higher stability due to the non-seasonal production processes (e.g., paper mill, brewery, semiconductor industry, etc.) might reduce the above-described limits. Finally, to progress towards the actual implementation EPS recovery-oriented solutions, the whole process of EPS extraction/valorization should be evaluated in terms of environmental and economic impacts (for instance by Life Cycle Assessment). To enhance the potential of WWTPs as WRRFs and improve the sustainability of the whole treatment chain, the EPS recovery as value-added biomaterials should be combined with an efficient management of the residual (i.e., non-extracted) waste sludge (e.g., anaerobic digestion of sludge residues for biomethane production).

4. Conclusions

Taking advantage of material-saving and reproducible experimental protocols, this study demonstrated that AGS-derived sEPS can form hydrogel-like materials with high-water content (up to 99 wt%) and versatile solid-like mechanical properties. This was confirmed by the strain and frequency dependence of G', G'' and η^* in oscillatory shear experiments. As a result of the higher complexity and diversity of the extracellular biopolymeric matrix, higher driving forces were needed to allow the establishment of an extended 3D hydrogel network (sEPS concentrations $\geq$ 2.5 wt%, $Ca^{2+} \geq$ 0.1 M) with respect to reference gelling biopolymers. However, as evidenced in compression–decompression studies, levels of elasticity and stiffness (E up to about 20 kPa under the tested conditions) comparable to other biopolymer-based systems currently applied for commercial purposes (e.g., ι-carrageenan) were observed, thus suggesting the promising development of sEPS-based biomaterials towards the broader implementation of WRRFs. Particularly, varying polymer concentration and (ionic) cross-linker concentration and nature it has been demonstrated the feasibility of forming hydrogels-based materials with distinct levels of stiffness and an almost unchanged mechanical behaviour, thus expanding the potential range of viable applications.

Declaration of competing interest

The authors declare that the content of this article is not subjected to conflict of interest.

Data availability

The authors are unable or have chosen not to specify which data has been used.

Acknowledgements

This work was supported by University of Toulouse – INSA Toulouse (Toulouse Biotechnology Institute, TBI) and University of Florence (Department of Civil and Environmental Engineering, DICEA). All authors thank N. Derlon (EAWAG – Swiss Federal Institute of Aquatic Science and Technology, Switzerland) who provided part of the aerobic granules used in the research activity.

Supplementary data

Supplementary data to this article can be found online at https://doi.org/10.1016/j.jwpe.2022.103076.

References

[1] M. Pronk, M.K. de Kreuk, B. de Bruin, P. Kamminga, R. Kleerebezem, M.C.M. van Loosdrecht, Full scale performance of the aerobic granular sludge process for sewage treatment, Water Res. 84 (2015) 207–217, https://doi.org/10.1016/j.watres.2015.07.011.

[2] R. Campo, S. Sguanci, S. Caffaz, L. Mazzoli, M. Ramazzotti, C. Lubello, T. Lotti, Efficient carbon, nitrogen and phosphorus removal from low C/N real domestic wastewater with aerobic granular sludge, Bioresour. Technol. 305 (2020), 122961, https://doi.org/10.1016/j.biortech.2020.122961.

[3] Y. Liu, J.H. Tay, State of the art of biogranulation technology for wastewater treatment, Biotechnol. Adv. 22 (2004) 533–563, https://doi.org/10.1016/j.biotechadv.2004.05.001.

[4] M.K. De Kreuk, C. Picioreanu, M. Hosseini, J.B. Xavier, M.C.M. Van Loosdrecht, Kinetic model of a granular sludge SBR: influences on nutrient removal, Biotechnol. Bioeng. 97 (2007) 801–815, https://doi.org/10.1002/bit.21196.

[5] T. Seviour, M. Pijuan, T. Nicholson, J. Keller, Z. Yuan, Understanding the properties of aerobic sludge granules as hydrogels, Biotechnol. Bioeng. 102 (2009) 1483–1493, https://doi.org/10.1002/bit.22164.

[6] G. Yilmaz, R. Lemaire, J. Keller, Z. Yuan, Simultaneous nitrification, denitrification, and phosphorus removal from nutrient-rich industrial wastewater using granular sludge, Biotechnol. Bioeng. 100 (2008) 529–541, https://doi.org/10.1002/bit.21774.

[7] Y. Lin, K.G.J. Nierop, E. Girbal-Neuhauser, M. Adriaanse, M.C.M. van Loosdrecht, Sustainable polysaccharide-based biomaterial recovered from waste aerobic granular sludge as a surface coating material, Sustain. Mater. Technol. 4 (2015) 24–29, https://doi.org/10.1016/j.susmat.2015.06.002.

[8] N. Derlon, J. Wagner, R.H.R. da Costa, E. Morgenroth, Formation of aerobic granules for the treatment of real and low-strength municipal wastewater using a sequencing batch reactor operated at constant volume, Water Res. 105 (2016) 341–350, https://doi.org/10.1016/j.watres.2016.09.007.

[9] M. Layer, M.G. Villodres, A. Hernandez, E. Reynaert, E. Morgenroth, N. Derlon, Limited simultaneous nitrification-denitrification (SND) in aerobic granular sludge systems treating municipal wastewater: mechanisms and practical implications, Water Res. X 7 (2020), 100048, https://doi.org/10.1016/j.wroa.2020.100048.

[10] W. Zhang, F. Jiang, Membrane fouling in aerobic granular sludge (AGS)-membrane bioreactor (MBR): effect of AGS size, Water Res. 157 (2019) 445–453, https://doi.org/10.1016/j.watres.2018.07.069.

[11] W. Zhang, W. Liang, Z. Zhang, T. Hao, Aerobic granular sludge (AGS) scouring to mitigate membrane fouling: performance, hydrodynamic mechanism and contribution quantification model, Water Res. 188 (2021), 116518, https://doi.org/10.1016/j.watres.2020.116518.

[12] H. Flemming, J. Wingender, The biofilm matrix, Nat. Publ. Group 8 (2010) 623–633, https://doi.org/10.1038/nrmicro2415.

[13] T. Seviour, Z. Yuan, M.C.M. van Loosdrecht, Y. Lin, Aerobic sludge granulation: a tale of two polysaccharides? Water Res. 46 (2012) 4803–4813, https://doi.org/10.1016/j.watres.2012.06.018.

[14] T. Seviour, N. Derlon, M.S. Dueholm, H. Flemming, E. Girbal-Neuhauser, H. Horn, S. Kjelleberg, M.C.M. van Loosdrecht, T. Lotti, F. Malpei, R.R. Nerenberg, T.R. Neu, E. Paul, H. Yu, Y. Lin, Extracellular polymeric substances of biofilms: suffering from an identity crisis, Water Res. 151 (2019) 1–7, https://doi.org/10.1016/j.watres.2018.11.020.

[15] H. Flemming, T.R. Neu, D.J. Wozniak, N. Carolina, A. Decho, J. Kreft, T. Neu, P. Nielsen, U. Ro, S. Schooling, U. Szewzyk, G. Wolfaardt, The EPS matrix: the "House of biofilm cells", J. Bacteriol. 189 (2007) 7945–7947, https://doi.org/10.1128/JB.00858-07.

[16] G.P. Sheng, H.Q. Yu, X.Y. Li, Extracellular polymeric substances (EPS) of microbial aggregates in biological wastewater treatment systems: a review, Biotechnol. Adv. 28 (2010) 882–894, https://doi.org/10.1016/j.biotechadv.2010.08.001.

[17] S. Felz, S. Al-Zuhairy, O.A. Aarstad, M.C.M. van Loosdrecht, Y. Lin, Extraction of structural extracellular polymeric substances from aerobic granular sludge, J. Vis. Exp. (2016) 1–8, https://doi.org/10.3791/54534.

[18] Y. Lin, M. de Kreuk, M.C.M. van Loosdrecht, A. Adin, Characterization of alginate-like exopolysaccharides isolated from aerobic granular sludge in pilot-plant, Water Res. 44 (2010) 3355–3364, https://doi.org/10.1016/j.watres.2010.03.019.

[19] K.I. Draget, G. Skjåk Bræk, O. Smidsrød, Alginic acid gels: the effect of alginate chemical composition and molecular weight, Carbohydr. Polym. 25 (1994) 31–38, https://doi.org/10.1016/0144-8617(94)90159-7.

[20] S. Felz, H. Kleikamp, J. Zlopasa, M.C.M. van Loosdrecht, Y. Lin, Impact of metal ions on structural EPS hydrogels from aerobic granular sludge, Biofilm 2 (2020), 100011, https://doi.org/10.1016/j.bioflm.2019.100011.

[21] S. de Valk, C. Feng, A.F. Khadem, J.B. van Lier, M.K. de Kreuk, Elucidating the microbial community associated with the protein preference of sludge-degrading worms, Environ. Technol. 40 (2019) 192–201, https://doi.org/10.1080/09593330.2017.1384071.

[22] M.C.M. van Loosdrecht, D. Brdjanovic, Anticipating the next century of wastewater treatment, Science 344 (2014) 1452–1453, https://doi.org/10.1126/science.1255183.

[23] S.B. Sam, E. Dulekgurgen, Characterization of exopolysaccharides from floccular and aerobic granular activated sludge as alginate-like-exoPS, Desalin. Water Treat. 57 (2016) 2534–2545, https://doi.org/10.1080/19443994.2015.1052567.

[24] N.K. Kim, N. Mao, R. Lin, D. Bhattacharyya, M.C.M. van Loosdrecht, Y. Lin, Flame retardant property of flax fabrics coated by extracellular polymeric substances recovered from both activated sludge and aerobic granular sludge, Water Res. 170 (2020), 115344, https://doi.org/10.1016/j.watres.2019.115344.

[25] I. Karakas, S.B. Sam, E. Cetin, E. Dulekgurgen, G. Yilmaz, Resource recovery from an aerobic granular sludge process treating domestic wastewater, J. Water Process Eng. 34 (2020), 101148, https://doi.org/10.1016/j.jwpe.2020.101148.

[26] D. Sudmalis, T.M. Mubita, M.C. Gagliano, E. Dinis, G. Zeeman, H.H.M. Rijnaarts, H. Temmink, Cation exchange membrane behaviour of extracellular polymeric substances (EPS) in salt adapted granular sludge, Water Res. 178 (2020), 115855, https://doi.org/10.1016/j.watres.2020.115855.

[27] G. Guibaud, D. Bhatia, P. d'Abzac, I. Bourven, F. Bordas, E.D. van Hullebusch, P.N. L. Lens, Cd(II) and Pb(II) sorption by extracellular polymeric substances (EPS) extracted from anaerobic granular biofilms: evidence of a pH sorption-edge, J. Taiwan Inst. Chem. Eng. 43 (2012) 444–449, https://doi.org/10.1016/j.jtice.2011.12.007.

[28] N. Li, D. Wei, S. Wang, L. Hu, W. Xu, B. Du, Q. Wei, Comparative study of the role of extracellular polymeric substances in biosorption of Ni(II) onto aerobic/anaerobic granular sludge, J. Colloid Interface Sci. 490 (2017) 754–761, https://doi.org/10.1016/j.jcis.2016.12.006.

[29] B. Pagliaccia, E. Carretti, M. Severi, D. Berti, C. Lubello, T. Lotti, Heavy metal biosorption by extracellular polymeric substances (EPS) recovered from anammox granular sludge, J. Hazard. Mater. 424 (2022), 126661, https://doi.org/10.1016/j.jhazmat.2021.126661.

[30] M.K. Lima-Tenório, E.T. Tenório-Neto, M.R. Guilherme, F.P. Garcia, C. V. Nakamura, E.A.G. Pineda, A.F. Rubira, Water transport properties through starch-based hydrogel nanocomposites responding to both pH and a remote magnetic field, Chem. Eng. J. 259 (2015) 620–629, https://doi.org/10.1016/j.cej.2014.08.045.

[31] A. Morales, J. Labidi, P. Gullón, G. Astray, Synthesis of advanced biobased green materials from renewable biopolymers, Curr. Opin. Green Sustain. Chem. 29 (2021), 100436, https://doi.org/10.1016/j.cogsc.2020.100436.

[32] P. Milani, D. França, A.G. Balieiro, R. Faez, Polymers and its applications in agriculture, Polimeros 27 (2017) 256–266, https://doi.org/10.1590/0104-1428.09316.

[33] S. Afridi, M.A. Sikandar, M. Waseem, H. Nasir, A. Naseer, Chemical durability of superabsorbent polymer (SAP) based geopolymer mortars (GPMs), Constr. Build. Mater. 217 (2019) 530–542, https://doi.org/10.1016/j.conbuildmat.2019.05.101.

[34] M.L. Oyen, Mechanical characterisation of hydrogel materials, Int. Mater. Rev. 59 (2014) 44–59, https://doi.org/10.1179/1743280413Y.0000000022.

[35] S. Thakur, B. Sharma, A. Verma, J. Chaudhary, S. Tamulevicius, V.K. Thakur, Recent progress in sodium alginate based sustainable hydrogels for environmental applications, J. Clean. Prod. 198 (2018) 143–159, https://doi.org/10.1016/j.jclepro.2018.06.259.

[36] C.K. Kuo, P.X. Ma, Ionically crosslinked alginate hydrogels as scaffolds for tissue engineering: Part 1. Structure, gelation rate and mechanical properties, Biomaterials 22 (2001) 511–521. PII: S0142-9612(00)00201-5.

[37] C.M. Schambeck, E. Girbal-Neuhauser, L. Böni, P. Fischer, Y. Bessière, E. Paul, R.H. R. da Costa, N. Derlon, Chemical and physical properties of alginate-like exopolymers of aerobic granules and flocs produced from different wastewaters, Bioresour. Technol. 312 (2020), 123632, https://doi.org/10.1016/j.biortech.2020.123632.

[38] K.Y. Lee, D.J. Mooney, Alginate: properties and biomedical applications, Prog. Polym. Sci. 37 (2012) 106–126, https://doi.org/10.1016/j.progpolymsci.2011.06.003.

[39] K.Y. Lee, S.H. Yuk, Polymeric protein delivery systems, Prog. Polym. Sci. 32 (2007) 669–697, https://doi.org/10.1016/j.progpolymsci.2007.04.001.

[40] B.E. Christensen, M. Indergaard, O. Smidsrød, Polysaccharide research in Trondheim, Carbohydr. Polym. 13 (1990) 239–255, https://doi.org/10.1016/0144-8617(90)90057-Y.

[41] J. Kozlowska, K. Pauter, A. Sionkowska, Carrageenan-based hydrogels: effect of sorbitol and glycerin on the stability, swelling and mechanical properties, Polym. Test. 67 (2018) 7–11, https://doi.org/10.1016/j.polymertesting.2018.02.016.

[42] T.R. Thrimawithana, S. Young, D.E. Dunstan, R.G. Alany, Texture and rheological characterization of kappa and iota carrageenan in the presence of counter ions, Carbohydr. Polym. 82 (2010) 69–77, https://doi.org/10.1016/j.carbpol.2010.04.024.

[43] C. Rochas, M. Rinaudo, Calorimetric determination of the conformational transition of kappa carrageenan, Carbohydr. Res. 105 (1982) 227–236, https://doi.org/10.1016/S0008-6215(00)84970-8.

[44] B. Frolund, T. Griebe, P.H. Nielsen, Enzymatic activity in the activated-sludge floc matrix, Appl. Microbiol. Biotechnol. 43 (1995) 755–761, https://doi.org/10.1007/BF00164784.

[45] C. Rondel, C.E. Marcato-Romain, E. Girbal-Neuhauser, Development and validation of a colorimetric assay for simultaneous quantification of neutral and uronic sugars, Water Res. 47 (2013) 2901–2908, https://doi.org/10.1016/j.watres.2013.03.010.

[46] E. Gómez-Ordóñez, P. Rupérez, FTIR-ATR spectroscopy as a tool for polysaccharide identification in edible brown and red seaweeds, Food Hydrocoll. 25 (2011) 1514–1520, https://doi.org/10.1016/j.foodhyd.2011.02.009.

[47] A. Banerjee, S. Ganguly, Mechanical behaviour of alginate film with embedded voids under compression-decompression cycles, Sci. Rep. 9 (2019) 1–12, https://doi.org/10.1038/s41598-019-49589-w.

[48] M. Ahearne, E. Siamantouras, Y. Yang, K.K. Liu, Mechanical characterization of biomimetic membranes by micro-shaft poking, J. R. Soc. Interface 6 (2009) 471–478, https://doi.org/10.1098/rsif.2008.0317.

[49] M. Watase, K. Nishinari, Rheological and thermal properties of carrageenan gels, effect of sulfate content, Macromol. Chem. 188 (1987) 2213–2221, https://doi.org/10.1002/macp.1987.021880918.

[50] S. Felz, P. Vermeulen, M.C.M. van Loosdrecht, Y. Lin, Chemical characterization methods for the analysis of structural extracellular polymeric substances (EPS), Water Res. 157 (2019) 201–208, https://doi.org/10.1016/j.watres.2019.03.068.

[51] S. Felz, T.R. Neu, M.C.M. van Loosdrecht, Y. Lin, Aerobic granular sludge contains hyaluronic acid-like and sulfated glycosaminoglycans-like polymers, Water Res. 169 (2020), 115291, https://doi.org/10.1016/j.watres.2019.115291.

[52] L. Zhu, J. Zhou, M. Lv, H. Yu, H. Zhao, X. Xu, Specific component comparison of extracellular polymeric substances (EPS) in flocs and granular sludge using EEM

and SDS-PAGE, Chemosphere 121 (2015) 26–32, https://doi.org/10.1016/j.chemosphere.2014.10.053.
[53] Y. Li, S.F. Yang, J.J. Zhang, X.Y. Li, Formation of artificial granules for proving gelation as the main mechanism of aerobic granulation in biological wastewater treatment, Water Sci. Technol. 70 (2014) 548–554, https://doi.org/10.2166/wst.2014.260.
[54] T. Seviour, M. Pijuan, T. Nicholson, J. Keller, Z. Yuan, Gel-forming exopolysaccharides explain basic differences between structures of aerobic sludge granules and floccular sludges, Water Res. 43 (2009) 4469–4478, https://doi.org/10.1016/j.watres.2009.07.018.
[55] I.D. Hay, Z.U. Rehman, M.F. Moradali, Y. Wang, B.H.A. Rehm, Microbial alginate production, modification and its applications, Microb. Biotechnol. 6 (2013) 637–650, https://doi.org/10.1111/1751-7915.12076.
[56] L. Cao, W. Lu, A. Mata, K. Nishinari, Y. Fang, Egg-box model-based gelation of alginate and pectin: a review, Carbohydr. Polym. 242 (2020), 116389, https://doi.org/10.1016/j.carbpol.2020.116389.
[57] I. Farrés, I.T. Norton, Formation kinetics and rheology of alginate fluid gels produced by in-situ calcium release, Food Hydrocoll. 40 (2014) 76–84, https://doi.org/10.1016/j.foodhyd.2014.02.005.
[58] I. Donati, Y.A. Mørch, B.L. Strand, G. Skjåk-Braek, S. Paoletti, Effect of elongation of alternating sequences on swelling behavior and large deformation properties of natural alginate gels, J. Phys. Chem. B 113 (2009) 12916–12922, https://doi.org/10.1021/jp905488u.
[59] I. Donati, F. Asaron, S. Paoletti, Experimental evidence of counterion affinity in alginates: the case of nongelling ion Mg2+, J. Phys. Chem. B 113 (2009) 12877–12886, https://doi.org/10.1021/jp902912m.
[60] C. Ouwerx, N. Velings, M.M. Mestdagh, M.A.V. Axelos, Physico-chemical properties and rheology of alginate gel beads formed with various divalent cations, Polym. Gels Networks 6 (1998) 393–408, https://doi.org/10.1016/S0966-7822(98)00035-5.
[61] L. Wei, J. Li, M. Xue, S. Wang, Q. Li, K. Qin, J. Jiang, J. Ding, Q. Zhao, Adsorption behaviors of Cu2+, Zn2+ and Cd2+ onto proteins, humic acid, and polysaccharides extracted from sludge EPS: sorption properties and mechanisms, Bioresour. Technol. 291 (2019), 121868, https://doi.org/10.1016/j.biortech.2019.121868.
[62] G.-F. Li, W.-J. Ma, Y.-F. Cheng, S.-T. Li, J.-W. Zhao, J.-P. Li, Q. Liu, N.-S. Fan, B.-C. Huang, R.-C. Jin, A spectra metrology insight into the binding characteristics of Cu2+ onto anammox extracellular polymeric substances, Chem. Eng. J. 393 (2020), 124800, https://doi.org/10.1016/j.cej.2020.124800.
[63] G.-P. Sheng, J. Xu, H.-W. Luo, W.-W. Li, W.-H. Li, H.-Q. Yu, Z. Xie, S.-Q. Wei, F.-C. Hu, Thermodynamic analysis on the binding of heavy metals onto extracellular polymeric substances (EPS) of activated sludge, Water Res. 47 (2013) 607–614, https://doi.org/10.1016/j.watres.2012.10.037.
[64] P. d'Abzac, F. Bordas, E. van Hullebusch, P.N.L. Lens, G. Guibaud, Effects of extraction procedures on metal binding properties of extracellular polymeric substances (EPS) from anaerobic granular sludges, Colloids Surf. B: Biointerfaces 80 (2010) 161–168, https://doi.org/10.1016/j.colsurfb.2010.05.043.
[65] K. Almdal, J. Dyre, S. Hvidt, O. Kramer, Towards a phenomenological definition of the term 'gel', Polym. Gels Networks 1 (1993) 5–17, https://doi.org/10.1016/0966-7822(93)90020-I.
[66] M. Gottlieb, C.W. Macosko, G.S. Benjamin, K.O. Meyers, E.W. Merrill, Equilibrium modulus of model poly(dimethylsiloxane) networks, Macromolecules 14 (1981) 1039–1046, https://doi.org/10.1021/ma50005a028.
[67] F.C. Mackintosh, J. Kas, P.A. Janmey, Elasticity of semi-flexible polymer networks, Phys. Rev. Lett. 75 (1995) 4425–4428, https://doi.org/10.1103/PhysRevLett.75.4425.
[68] T. Lotti, E. Carretti, D. Berti, C. Montis, S. Del Buffa, C. Lubello, C. Feng, F. Malpei, Hydrogels formed by anammox extracellular polymeric substances: structural and mechanical insights, Sci. Rep. 9 (2019) 1–9, https://doi.org/10.1038/s41598-019-47987-8.
[69] A. Durmus, A. Kasgoz, C.W. Macosko, Linear low density polyethylene (LLDPE)/clay nanocomposites. Part I: structural characterization and quantifying clay dispersion by melt rheology, Polymer 48 (2007) 4492–4502, https://doi.org/10.1016/j.polymer.2007.05.074.
[70] K. Ueno, K. Hata, T. Katakabe, M. Kondoh, M. Watanabe, Nanocomposite ion gels based on silica nanoparticles and an ionic liquid: ionic transport, viscoelastic properties, and microstructure, J. Phys. Chem. B 112 (2008) 9013–9019, https://doi.org/10.1021/jp8029117.
[71] P.G. de Gennes, On a relation between percolation theory and the elasticity of gels, J. Phys. Lett. 37 (1976) 1–2, https://doi.org/10.1051/jphyslet:019760037010100.
[72] D. Stauffer, Gelation in concentrated critically branched polymer solutions, J. Chem. Soc. Faraday Trans. 272 (1976) 1354–1364, https://doi.org/10.1039/F29767201354.
[73] D. Stauffer, Introduction to Percolation Theory, Taylor and Francis, London, 1985.
[74] J.M. Guenet, Structure versus rheological properties in fibrillar thermoreversible gels from polymers and biopolymers, J. Rheol. 44 (2000) 947–960, https://doi.org/10.1122/1.551121.
[75] R. Zallen, The Physics of Amorphous Solids, Wiley, New York, 1983. Chapter 4.
[76] T. Funami, Y. Fang, S. Noda, S. Ishihara, M. Nakauma, K.I. Draget, K. Nishinari, G. O. Phillips, Rheological properties of sodium alginate in an aqueous system during gelation in relation to supermolecular structures and Ca2+ binding, Food Hydrocoll. 23 (2009) 1746–1755, https://doi.org/10.1016/j.foodhyd.2009.02.014.
[77] H. Bessaies-Bey, K.H. Khayat, M. Palacios, W. Schmidt, N. Roussel, Viscosity modifying agents: key components of advanced cement-based materials with adapted rheology, Cem. Concr. Res. 152 (2021), 106646, https://doi.org/10.1016/j.cemconres.2021.106646.
[78] E.S. Abdel-Halim, H.E. Emam, M.H. El-Rafie, Utilization of hydroxypropyl cellulose and poly(acrylic acid)-hydroxypropyl cellulose composite as thickeners for textile printing, Carbohydr. Polym. 74 (2008) 938–941, https://doi.org/10.1016/j.carbpol.2008.05.013.
[79] L. Passauer, T. Hallas, E. Ba, G. Ciesielski, S. Lebioda, U. Hamer, Biodegradation of hydrogels from oxyethylated lignins in model soils, ACS Sustain. Chem. Eng. 3 (2015) 1955–1964, https://doi.org/10.1021/acssuschemeng.5b00139.